

Supplementary Information for

A heated rock crack captures and polymerizes primordial DNA and RNA

Christina F. Dirscherl, Alan Ianeselli, Damla Tetiker, Thomas Matreux, Robbin M. Queener, Christof B. Mast and Dieter Braun*

Systems Biophysics and Center for NanoScience, Ludwigs-Maximilians-Universität München, 80799 Munich, Germany

*Dieter Braun: dieter.braun@lmu.de , ORCID: 0000-0001-7751-1448

This PDF file includes:

Supplementary Information Text Sections I to XII
Figures S1 to S16
Tables S1 to S7
Legends for Movies S1 to S6
Legends for Datasets S1 to S6
SI-References

Other supplementary materials for this manuscript include the following:

Movies S1 to S6
Datasets S1 to S6
(Can be downloaded from: Dirscherl, Christina Felicitas and Braun, Dieter: *Supplementary Datasets for the Paper "A heated rock crack captures and polymerizes primordial DNA and RNA"*. 2022. Open Data LMU. DOI: <https://data.ub.uni-muenchen.de/351/>)

Supplementary Information Text

I. CHEMICAL PROCEDURES

1. AlmpdA Synthesis

3.3 mmole (1 eq) deoxythymidine-5'-monophosphate disodium salt (dTMPNa₂, CAS No. 33430-62-5, Carbosynth Ltd.) and 16.4 mmole (5 eq) 2-aminoimidazole sulfate salt (SKU No. 197912-2.5G, Sigma Aldrich) were dissolved in 25 mL of RNase-free water (Ambion TM Nuclease-Free Water, Ref. No. AM 9932, Life Technologies Corporation) in a 50 mL polypropylene Falcon tube. The pH was adjusted to 5.7 by adding a solution of syringe-filtered 1 M hydrogen chloride (HCl, Art. No. K025.1, Carl Roth GmbH + Co. KG). RNase-free water was added to give a total volume of 30 mL. The mixture was filtered with a 0.45 µm filter and aliquoted into two 50 mL polypropylene Falcon tubes, flash-frozen in liquid nitrogen, and lyophilized for two days.

In 250 mL glass round-bottom flasks, a mixture of 50 mL anhydrous dimethyl sulfoxide (SKU No. 276855-1L, Sigma-Aldrich) and 6.2 mL anhydrous triethylamine (CAS No. 121-44-8, Carl Roth GmbH + Co. KG) was stirred under argon. The lyophilized products were added and heated gently in a flame for 30 min. To each flask, 29.5 mmole (9 eq) triphenylphosphine (TEA, CAS No. 603-35-0, Carl Roth GmbH + Co. KG COMPANY) and 32.8 mmole (10 eq) 2,2'-dipyridyldisulfide (SKU No. 8411090005, Sigma-Aldrich) were added. The mixtures were stirred under argon for 30 min. The solutions were poured in an ice-cooled glass bottle containing a mixture of 400 mL acetone (UN No. 1019, Carl Roth GmbH + Co. KG), 250 mL diethyl ether (CAS No. 60-29-7 Carl Roth GmbH + Co. KG company), 30 mL trimethylamine (UN No. 1296, Carl Roth GmbH + Co. KG) and 1.6 mL acetone saturated with sodium perchlorate (NaClO₄) (SKU No. 410241-500G, Sigma-Aldrich), and stirred until the product flocculated.

Stirring was stopped and the bottle was put on ice for 30 min. The solution was collected in 50 mL polypropylene Falcon tubes and centrifuged at 4000 rpm for 3 min at 10°C. The supernatant was discarded and the pellets were resuspended in 10 mL of a 1 : 8.3 : 13.3 of triethylamine : diethyl ether : acetone mixture. The new solutions were vortexed and centrifuged at 4000 rpm for 3 min at 10°C. The supernatant was discarded, and the step was repeated. The pellet was washed twice with 10 mL acetone and twice with 10 mL diethyl ether. The pellets were dried overnight under vacuum. The product was stored at -20°C.

2. AlmpdA Polymerization

For an experiment, the self-synthesized AlmpdA powder was allowed to thaw to room temperature, weighed, put into a low-binding test tube (DNA LoBind® Tubes, Eppendorf AG), and mixed with a 100 mM 3-(N-morpholino)propanesulfonic acid (MOPS) buffer solution (CAS No. [1132-61-2], Carl Roth GmbH + Co. KG mixed with RNase-free water) to the desired concentration (300 mM, 30 mM, 2.5 mM). No other salts were added. The pH was not adjusted, it naturally settled at pH 6.5.

The sample mixture was filled into a thermophoretic pore, which had beforehand been filled with low viscosity oil (3M TM Novec TM 7500, IoLiTec Ionic Liquids Technologies GmbH) to allow complete filling of the pore without introducing any air bubbles. Novec Oil was checked in a separate experiment to not change the polymerization behavior, the filling procedure can be observed in the SI-Movie S1. The pore was operated for 24 h at a temperature gradient of $\Delta T = 22^\circ\text{C}$, with the hot temperature at 30°C and the cold temperature at 8°C at the front and back of the solution. For the bulk controls, 20 µl of sample was filled in Eppendorf test tubes and covered with 15 µl of paraffin oil (Art. No. 9190.1, Carl Roth GmbH + Co. KG) to prevent any evaporation inside the test tube. Paraffin oil was checked in a separate experiment to not change the polymerization behavior. The tubes were incubated for 24 h at 30°C and 8°C, respectively.

3. dAMP Accumulation

For each experiment, deoxyadenosine-5'-monophosphate disodium salt (dAMPNa₂, CAS No. 2922-74-9, Carbosynth Ltd.) powder was allowed to thaw to room temperature, weighed into a low-binding test tube and mixed with a 100 mM 3-(N-morpholino)propanesulfonic acid (MOPS) buffer solution to the desired concentration (300 mM, 20 mM, 2.5 mM). No other salts were added. The pH was not adjusted, it naturally settled at pH 6.5.

The sample mixture was filled into a thermophoretic pore, which had beforehand been filled with low viscosity oil (3M TM Novec TM 7500, IoLiTec Ionic Liquids Technologies GmbH) to allow complete filling of the pore without introducing any air bubbles. Novec oil was checked in a separate experiment to not change the polymerization behavior, the filling procedure can be observed in the SI-Movie S1. The pore was operated for 24 h at a temperature gradient of $\Delta T = 22^\circ\text{C}$, with the hot temperature at 30°C and the cold temperature at 8°C at the front and back of the solution.

4. 2'3'cyclic Polymerization

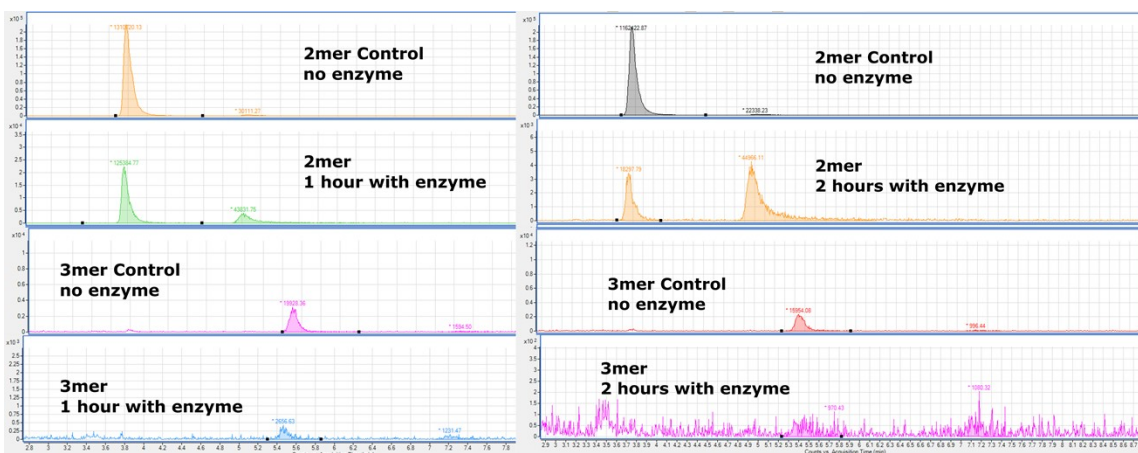
2'3'cCMP (Na-salt form, CAS No. 15718-51-1, Sigma-Aldrich) and 2'3'cGMP (Na-salt form, Cat. No. G025-50, Biolog Life Science Institute GmbH & Co. KG) were mixed with RNase-free water to create a stock solution of 300 mM. These stocks were stored at -80°C .

For an experiment, the stock solutions were diluted with RNase-free water to the desired concentrations and G/C ratios (10 mM/50 mM, 1 mM/5 mM, 20 mM/20 mM, 2 mM/2 mM). The pH of the solution was adjusted to 10.5 with potassium hydroxide (KOH, Art. No. K017.1, Carl Roth GmbH + Co. KG). If visualization of the accumulation process was desired, 10 μM Cy5 fluorescent dye (Cat. 23390, Lumiprobe GmbH, excitation maximum: 649 nm, emission maximum: 666 nm) were added, which was tested in a separate experiment not to change the polymerization behavior (data not shown).

The sample mixture was filled into an air-filled thermophoretic pore from its top until it filled the upper 4/5 of the chamber volume, the lowest fifth was left air-filled to create the liquid-gas interface. The filling procedure with an air-water interface is shown in SI-Movie S2. The pore was operated for 18 h at a temperature gradient of $\Delta T = 30^\circ\text{C}$, with the hot temperature at 70°C and the cold temperature at 40°C . For the dry control, 20 μl of the sample was filled in test tubes and incubated for 18 h at 40°C and 70°C , respectively, with the tube lid open to allow evaporation. After the 18 h, samples were rehydrated with 20 μl of RNase-free water. For bulk controls, 20 μl of sample was filled in test tubes and covered with 15 μl of low viscosity paraffin oil (CAS No. 8042-47-5, Carl Roth GmbH + Co. KG) to prevent any evaporation inside the test tube. Paraffin oil was checked in a separate experiment to not change the polymerization behavior. The tubes were kept with closed lids for 18 h at 40°C and 70°C , respectively.

5. Pyrophosphatase Enzyme Digestion Protocol

We used the NudC Pyrophosphatase Kit (M0607S, New England BioLabs Inc.) for digestion of pyrophosphate-linkages in our AlmpdA-polymerization products. After 24h of incubation at 20°C in a test tube, 15 μl of a 2.5mM-AlmpdA sample were mixed in a new test tube with the following chemicals, all included in the kit: 2 μl NEBuffer 3.1 (10x), 1 μl 100 mM DTT (dithiothreitol) and 2 μl NudC pyrophosphatase (10 μM). The tube was vortexed, spun down and incubated for either 1 h or 2 h at 37°C . Without further treatment, we measured the digested sample with the same HPLC-MS protocol as the undigested sample (see SI-section IV.2) and compared the results of both measurements. Data and analysis are shown in SI-Fig. S1 and SI-Tab. S1.



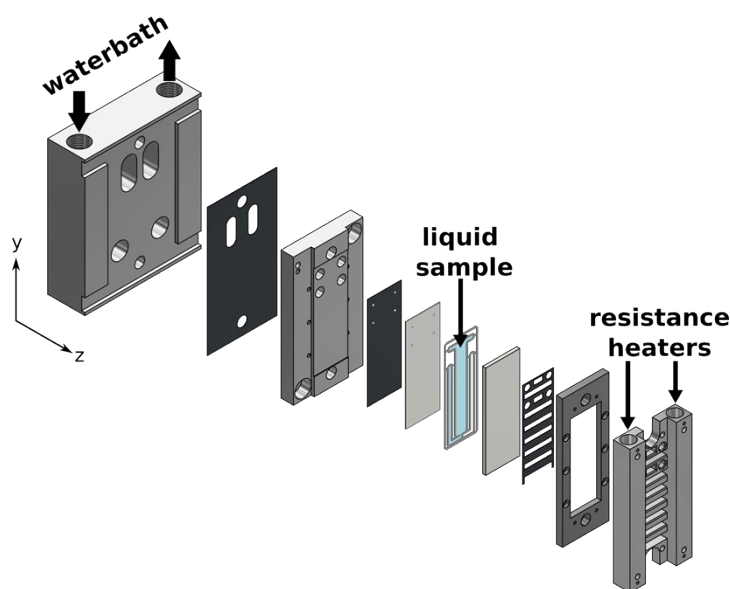
SI-FIG. S1. Identification of the pyrophosphate-oligomer peaks by a pyrophosphatase enzyme digestion protocol. 15 μ l of an AlmpdA-polymerization sample were incubated for 1 h with a pyrophosphatase enzyme, which hydrolyzes pyrophosphate bonds in oligomers and cleaves them into shorter, linear oligomers (see SI-section I.5 for enzyme digestion protocol). Then, both the digested and the undigested samples were measured and extracted by HPLC-MS and MassHunter. The peak of the linear oligomer was identified by comparison with a commercially available standard (see SI-Fig. S8) for 2mer and 3mer. The first peak in the 2mer- and 3mer-chromatograms, with the same mass but an earlier retention time, shrank in integrated area counts when incubated with a pyrophosphatase enzyme, while the second, linear peak grew. The same result, but more pronounced, was observed in a second experiment in which we incubated another AlmpdA-polymerization sample for 2 h with the pyrophosphatase enzyme. Hence, we concluded that the peaks which decreased in area indeed contained the pyrophosphate-linked oligomers. The linear peaks (at later retention times) grew because the pyrophosphatase enzyme cleaved longer pyrophosphate-oligomers to form shorter, linear oligomers, which then appeared in the linear peaks of the chromatograms of the shorter oligomers and increased the integrated area counts there. The integrated area counts of the decreasing and increasing peaks are given in SI-Tab. S1.

Oligomer Length	Protocol	Area Pyrophosphate Peak	Area Linear Peak
2mers	Control	1310720	30111
	1h enzyme digestion	125385	43831
	Control	1162422	22338
	2h enzyme digestion	18297	44966
3mers	Control	19928	1594
	1h enzyme digestion	2656	1231
	Control	15954	996
	2h enzyme digestion	970	1080

SI-TAB. S1. Integrated area counts for decreasing and increasing peaks of AlmpdA-polymerization products before and after pyrophosphatase enzyme digestion. Two enzyme digestion experiments were performed in which we incubated 15 μ l of an AlmpdA-polymerization sample for 1 h or 2 h with a pyrophosphatase enzyme. The increase and decrease of the areas of a peak denoted whether the amount of measured products in that peak was higher or lower after the digestion protocol. We saw that the areas of the pyrophosphate peaks shrank, while the area counts of the linear peaks increased after the enzyme digestion (see SI-Fig. S1). Thus, we had evidence that the peaks we called pyrophosphate peaks indeed contained the pyrophosphate-linked oligomers from the AlmpdA-polymerization reaction and the pyrophosphatase enzyme cleaved them into shorter, linear oligomers.

II. DETAILS OF THE MICROFLUIDIC CHAMBER AND THE EXPERIMENTAL SETUP

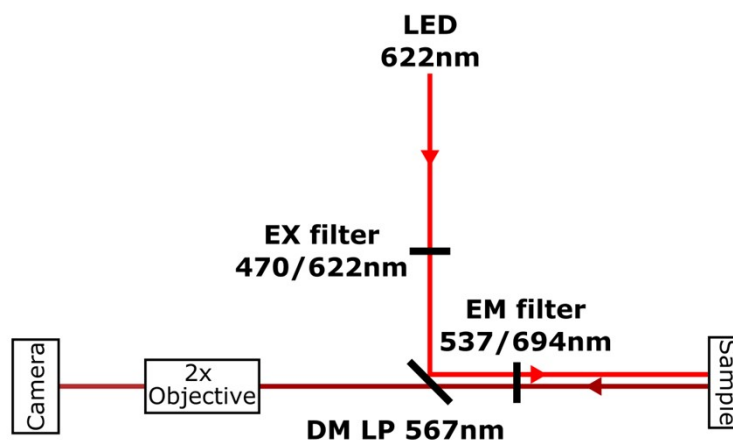
The non-equilibrium experiments were performed in a chamber ($170\ \mu\text{m} \times 7\ \text{mm} \times 52\ \text{mm}$, total volume: $62\ \mu\text{l}$) cut from a thin Teflon foil ($170\ \mu\text{m}$ thickness, FEP-Teflon, Holscot, Netherlands) and was placed between a transparent cooled back sapphire of $0.5\ \text{mm}$ thickness (with four laser-cut holes of $1\ \text{mm}$ diameter, Kyburz, Switzerland) and a heated front sapphire of $2\ \text{mm}$ thickness (no holes, Kyburz, Switzerland). The shape of the Teflon foil was designed in Inventor (Autodesk) and cut with a cutting plotter (CE6000-40 Plus, Graphtec). The sapphires were lined with two heat-conducting graphite foils (one of $25\ \mu\text{m}$ thickness in the back, EYGS091203DP, $1600\ \text{W/mK}$, Panasonic, one of $200\ \mu\text{m}$ thickness in the front, EYGS0811ZLGH, $400\ \text{W/mK}$, Panasonic) to ensure a good thermal connection to an aluminum plate at the back and to the resistance rod heaters at the front. The layers were screwed with a steel frame to the back plate with a torque of $0.2\ \text{Nm}$, the heater was screwed to the front sapphire with a torque of $0.16\ \text{Nm}$. This sandwich is screwed to a waterbath-cooled (TXF200, Grant Instruments (Cambridge) Ltd) second aluminum block with a torque of $0.5\ \text{Nm}$ and with another $200\ \mu\text{m}$ thick graphite foil in between. All aluminum parts were designed in Inventor and fabricated in the university workshop. Four microfluidic teflon tubings (KAP 100.969, Techlab) were connected with fittings and ferrules (VBM 100.823 and VBM 100.632, Techlab) to the sapphire back wall of the chamber, which has four holes of $1\ \text{mm}$ diameter. These tubings served as inlet and outlet for the introduction of the liquid sample. A schematic of the chamber build-up is shown in SI-Figure S2. The process of building a pore can be observed in SI-Movie S3.



SI-FIG. S2. Schematic of the chamber. From left to right: waterbath-cooled aluminum block, heat conducting graphite foil ($200\ \mu\text{m}$ thickness), aluminum back plate, heat conducting graphite foil ($25\ \mu\text{m}$ thickness), bottom sapphire ($0.5\ \text{mm}$ thickness) with holes, Teflon cutout ($170\ \mu\text{m}$) containing the liquid sample, top sapphire ($2\ \text{mm}$ thickness), heat conducting graphite foil ($200\ \mu\text{m}$ thickness), steel frame for fixing the sapphire-teflon-sapphire sandwich on the back plate, aluminum element holding the resistance rod heaters.

For the dAMP and the AlmpdA experiments, the waterbath (50/50 water/ethylene-glycol) was set to -30°C and the resistance heaters to 80°C . For the 2'3'cyclic experiments, the waterbath was set to -20°C and the resistance heaters to 100°C . To calculate the inner temperatures of the chambers, we measured the temperatures on the outside of the sapphires with a temperature sensor (GTF 300, Greisinger) and a thermometer (GTH 1170 Typ K, Greisinger) and used the steady-state linear heat equation and the conductivities of water $0.60\ \text{W/mK}$ (at 20°C) and sapphire $23\ \text{W/mK}$ to calculate what temperature this translates to on the inside of the pore. For easy calculation for the reader, a self-coded LabVIEW program is provided in Dataset S2 (ThermalGradientCalculator.vi).

The fluorescent microscopy setup consisted of a standard fluorescence microscope (Axiotec, Carl Zeiss Microscopy Deutschland GmbH) equipped with an LED (622 nm, ThorLabs), a dual excitation filter (470 nm/622 nm), a dual emission filter (537 nm/694 nm), a dual band beamsplitter (497 nm/655 nm), a 2x objective (TL2x-SAP, 2x/0.1/350-700 nm/inf/WD 56.3 mm, ThorLabs) and a Stingray-F145B ASG camera (ALLIED Vision Technologies GmbH). A self-coded program using the software LabVIEW was used to control the camera and the output voltage to the LED and to the resistance heaters. A cartoon of the setup is shown in SI-Fig. S3.



SI-FIG. S3. Schematic of the fluorescent microscopy setup.

Light from an LED with wavelength 622 nm went through an excitation filter (622 nm) and onto a longpass dichroic mirror (567 nm), reflecting the light onto the sample. The emitted light went through an emission filter (694 nm), passed the dichroic mirror and a 2x objective and was recorded by a CCD camera.

III. FREEZE EXTRACTION AND SAMPLE PREPARATION

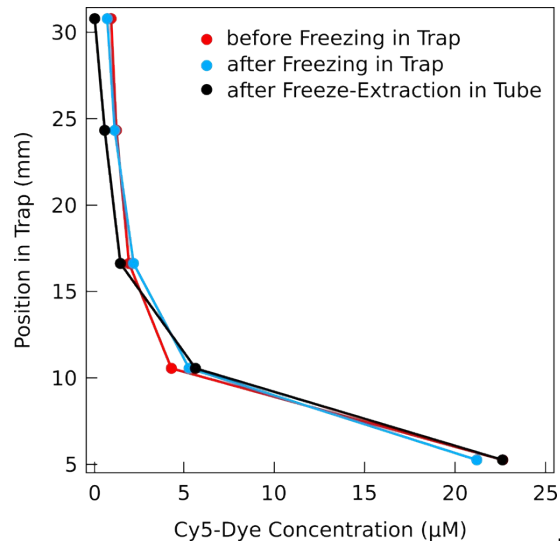
We developed a method to differentially extract all sections of the concentration gradient generated by the pore to study the processes of our combined physicochemical non-equilibrium system.

After the run time of the reaction in the thermal gradient, we turned off the front heating, which led to a rapid drop in temperature and finally to freezing of the pore contents as the waterbath was maintained at -30°C or -20°C respectively. After verifying by microscopy that the liquid contents were frozen, we removed the entire pore from the setup and placed it in the -80°C freezer for 30 min and unscrewed the sapphire-teflon-sapphire sandwich from the metal holders. The sandwich was placed on an aluminum block cooled to -80°C to prevent melting. The sandwich was opened, and the Teflon was removed using a razor blade. Only the frozen liquid content remained on the sapphires. We cut this into five stripes (for experiments of Fig. 1 and Fig. 2) or three stripes (for experiments of Fig. 3) of similar volume and slid the sapphire stripe by stripe over onto a 45°C aluminum block to melt the frozen sample stripe by stripe. To ensure that two adjacent stripes were not inadvertently mixed during the stripwise thawing, we held a hydrophobic barrier (glass cover slide wrapped with Teflon foil) between each stripe. The contents of each thawed stripe were pipetted into different low-binding Eppendorf tubes. After completion of the freeze extraction, the tubes were briefly centrifuged, their liquid contents were weighed, and the percentage of volume to the stripes to the total extracted volume of the pore was calculated. Then, the pH of the samples was measured with Orion VersaStar Pro pH-meter (ThermoFisher Scientific). The process of freeze extraction can be observed in SI-Movie S4 and seen in SI-Figure 4.



SI-FIG. S4. Photo of the freeze extraction process. The sapphire with the frozen sample was slid stripe by stripe over onto a 45°C warm aluminum block to melt the frozen sample stripe by stripe. To ensure that two adjacent stripes were not inadvertently mixed during the stripwise thawing, a hydrophobic barrier (glass cover slide wrapped with Teflon foil) was held between each stripe. The contents of each thawed stripe were pipetted into different low-binding Eppendorf tubes

We verified that the freezing process did not disturb the accumulation state of the pore by measurements with fluorescent Cy5-dye (see SI-Fig. S5).



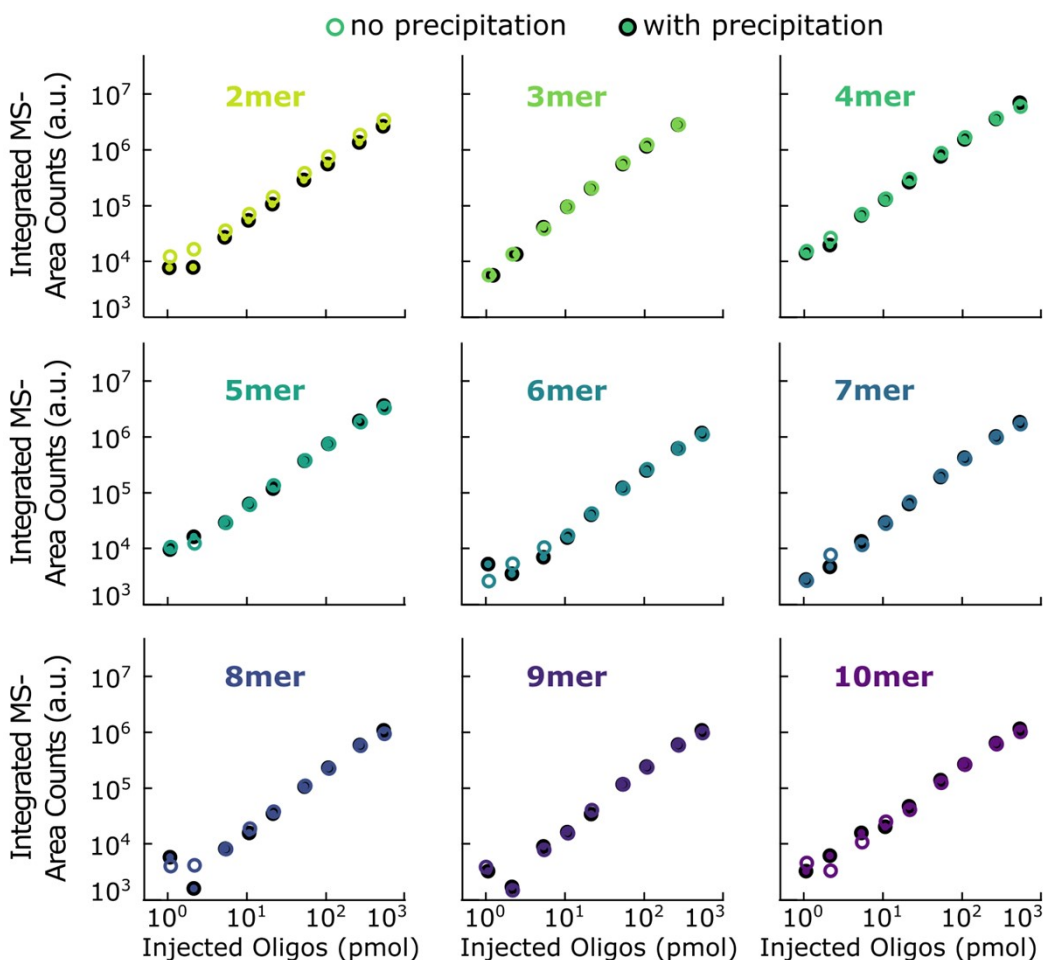
SI-FIG. S5. The process of freeze extraction did not disturb the concentration distribution of an accumulated pore. 10 µM fluorescent Cy5-dye in water was accumulated in a pore of 170 µm thickness for 4 h with a temperature gradient of $\Delta T = 30^\circ\text{C} - 8^\circ\text{C} = 22^\circ\text{C}$. Then, the freeze extraction steps described above were performed on this pore. For each step of the process, the concentration of the Cy5-dye was determined via fluorescence microscopy and thickness normalization for each cutout stripe content. We see that the freeze extraction process did not disturb the accumulation state of the pore, as all concentrations stay the same before and after freezing in the pore as well as after freeze extraction.

For the experiments of Fig. 1 and Fig. 2 in the main text, the samples were injected directly into the HPLC-MS system without further treatment. For the experiments of Fig. 3 of the main text, the samples were precipitated prior to measurement.

For the precipitation, 10 μ l of sample were mixed with 90 μ l RNase-free H₂O, 2 μ l of 10 mg/ml glycogen from oyster (G8751-5G, Sigma-Aldrich) and 10 μ l of 5 M Ammonium acetate (CAS 631-61-8, Sigma-Aldrich), then vortexed and spun down. 336 μ l of -20°C cold ethanol (Art-Nr. 5054.2, Carl Roth GmbH + Co. KG) was added, the mixture was vortexed, spun down and stored overnight in a 4°C fridge. The next day, the reaction tubes were centrifuged at 15000 rpm for 30 min at 4°C, the supernatant was discarded. 100 μ l of -20°C cold 70/30 ethanol/RNase-free water mixture were added. The tubes were centrifuged again at 15000 rpm for 30 min at 4°C.

The supernatant was pipetted off as thoroughly as possible and without further drying the pellet was then dissolved in 40 μ l of RNase-free water. Of this, 38 μ l were injected for HPLC-MS measurement in order to make sure to not inject air into the column.

With commercial standards over three orders of magnitude and for oligomer lengths from 2 nt to 10 nt we verified that the precipitation did not disturb the composition of the sample (see SI-Fig. S6).



SI-FIG. S6. Ethanol Precipitation of RNA does not Change the Strand Composition Commercially available 2-8mer polyG oligomers (3'-P-G...G-5', 3'-phosphate biomers.net GmbH, with HPLC purification) with known amounts (1 pmol, 2 pmol, 5 pmol, 10 pmol, 20 pmol, 50 pmol, 100 pmol, 250 pmol, 500 pmol in water) were measured with HPLC/ESI-TOF before and after ethanol precipitation as described in SI-Section III. The graphs for the different oligomer lengths above show that the same amount of oligomers before and after precipitation cause the same integrated MS area counts. Hence, the ethanol precipitation treatment does not change the composition of a sample for none of the examined lengths nor concentrations.

IV. HPLC-MS MEASUREMENT METHODS

The HPLC-MS measurements were performed using a time-of-flight mass spectrometer (TOF-MS) with an electrospray ion source (G6230BA, Agilent Technologies) and a 1260 Infinity II Bioinert high performance liquid chromatograph (HPLC, G5654A, Agilent Technologies). The column was an AdvancedBio Oligonucleotides column (4.6 × 150 mm, 2.7 Micron, P.N. 653950-702, Agilent Technologies) and the MS measurements were run in negative mode. For the liquid phase, we used as eluent A: UHPLC-water (CAS No. 7732-18-5, Supelco, Merck KGaA) with 200 mM 1,1,1,3,3,3-Hexafluor-2-propanol (HFIP, Art-Nr 2473.3, Carl Roth GmbH + Co. KG) and 8 mM TEA (CAS No. 603-35-0, Carl Roth GmbH + Co. KG COMPANY) and as eluent B: 50/50 UHPLC-water/methanol (CAS-No 67-56-1, Merck KGaA) with 200 mM HFIP and 8 mM TEA.

1. dAMP Accumulation

The injection volume was 2 µl for each sample, and the compressibility was set to 40×10^{-6} L/bar. A flow of 0.6 ml/min was maintained throughout the 40 min of the method. The column temperature was 30°C and the eluent gradients were 0.0 min: 79.0 % A 21.0 % B, 23.0 min: 53.0 % A 47.0 % B, 23.1 min: 0.0 % A 100.0 % B, 30.0 min: 0.0 % A 100.0 % B, 30.1 min: 79.0 % A 21.0 % B, 40.0 min: 79.0 % A 21.0 % B. The recorded diode array detector (DAD) signal was set to 259 nm with a bandwidth of 4 nm.

The measured mass range (m/z) was 320 u – 3200 u with a scan rate of 3 spectra/sec. The settings were: sheath gas flow: 11 L/min, sheath gas temperature: 400°C, nebulizer: 45 psig, gas flow: 5 L/min, gas temperature: 325°C, octupole RF-peak voltage: 800 V, skimmer voltage: 65 V, fragmentor voltage: 250 V, nozzle voltage: 2000 V, V-cap voltage: 4000 V. The reference masses were 1033.988109 u and 1333.968947 u (commercially available from Agilent).

2. AlmpdA Polymerization

The method was almost the same as for the dAMP accumulation experiments, except for the mass range, which excluded the monomer masses to obtain a cleaner ion chromatogram with lower background: mass range 550 u – 3200 u. Other minor changes were the gas flow: 8 L/min and the gas temperature: 300°C.

3. 2'3'cyclic Monomer Polymerization

The injection volume was 38 µl for each sample, and the compressibility was set to 50×10^{-6} L/bar. A flow of 1.0 ml/min was maintained throughout the 53 min of the method. The column temperature was 60°C and the eluent gradients were 0.0 min: 99.0 % A 1.0 % B, 5.0 min: 99.0 % A 1.0 % B, 27.5 min: 70.0 % A 30.0 % B, 42.5 min: 60.0 % A 40.0 % B, 42.6 min: 0.0 % A 100.0 % B, 47.5 min: 0.0 % A 100.0 % B, 47.6 min: 99.0 % A 1.0 % B, 53.0 min: 99.0 % A 1.0 % B. The recorded DAD signal was set to 260 nm with a bandwidth of 4 nm.

The measured mass range (m/z) was 500 u – 3200 u with a scan rate of 1 spectrum/sec. The settings were: sheath gas flow: 11 L/min, sheath gas temperature: 400°C, nebulizer: 45 psig, gas flow: 8 L/min, gas temperature: 325°C, octupole RF-peak voltage: 750 V, skimmer voltage: 65 V, fragmentor voltage: 175 V, nozzle voltage: 2000 V, V-cap voltage: 3500 V. The reference masses were 601.978977 u, 1033.988109 u and 1333.968947 u (commercially available from Agilent).

V. PEAK ANALYSIS AND CONCENTRATION CALIBRATION

After measurement by HPLC-MS, the masses of the polymerization products were extracted from the raw MS data and plotted in single chromatograms (ion count vs. time) with the Agilent software MassHunter Qualitative Analysis. We extracted the mass of the most abundant isotope of the molecule calculated by the Agilent Isotope Distribution Calculator (mass lists and chemical

formulas of the polymerization products, see SI-Chapter VI). For the ion extraction algorithm, we tolerated a symmetric margin of error of $\Delta m/z = \pm 2.0$ ppm around the target m/z values. Peak identification for integration was performed by comparing the retention times of the peaks of the sample with the retention times of the peaks from commercially available standards, enzyme digestion protocol, or hydrolysis experiments. We additionally verified that the selected peaks corresponded to the correct molecule by checking the isotope distribution signature of the peak in the first charge state (see SI-Chapter VI for isotope distributions). The selected peaks were integrated and the background was subtracted either manually using the MassHunter Qualitative Analysis program or with a self-coded LabVIEW program. To retrieve the concentration information from the integrated peak areas, a calibration procedure was used, which is described below.

1. dAMP Accumulation

The dAMP peak in the sample was identified by comparison with the retention times of an injection of commercially available dAMP in water. The selected peaks were integrated manually using the MassHunter Qualitative Analysis program. To remove the baseline noise, we performed a background subtraction. For that, an injection of RNase-free water was measured along with the samples. Then, the dAMP mass was also extracted from the water injection as described above and its chromatogram was integrated in the same time interval as the dAMP peaks of the samples. The resulting integration value was subtracted as background from the integrated area values of the corresponding sample peaks.

For calibration, the mass spectrometry data of monomers were measured over a wide range of concentrations (0.01 mM, 0.05 mM, 0.1 mM, 0.5 mM, 1 mM, 5 mM, 10 mM, 20 mM, 50 mM, 100 mM, 200 mM, 500 mM, 700 mM in 100 mM MOPS at pH 6.5), then extracted and integrated as described above. The integrated peak area increased with increasing concentration.

Due to the broad measurement range the peak area vs. concentration plots had to be fitted in two ranges, 0.01-20mM and 20-700mM (see SI-Fig. S6). For the concentration range 0.01-20mM, the fit function was a power-law

$$A(c)/F = y_0 + b \cdot c^{pow}$$

where

- A is the area of the integrated peak, c the concentration of the monomer related to this peak on the day of the measurement and F is a correction factor.
- $y_0 = -763470$, $b = 7095700$ and $pow = 0.565$ are fitting parameters determined by least square fitting.

To account for variations in the measurement performance of the HPLC-MS machine between different days (differences in the integrated peak area for the same oligomer concentration injection between days, see SI-Fig. S7), we introduced the correction factor F . F is given by the ratio of the integrated peak area of a 20 mM monomer injection measured on a measurement day $A_{20mMStd}^{today}$ divided by the integrated peak area value of a 20 mM monomer injection measured on the day of calibration $A_{20mMStd}^{Calib} = 56604517$. F was calculated anew on each measurement day by measuring a 20 mM standard monomer sample before measuring the actual experimental samples. The integrated peak area of a sample measured on a measurement day was divided by F to correct it to the value it would have had on the day of calibration. By inverting this equation to

$$c(A) = \left[\frac{\frac{A}{F} + 763470}{7095700} \right]^{1.77}$$

we could now calculate the concentration $c(A)$ from the area A of a peak.

For the concentration range 20-700 mM we used the same methods, but a different fit function

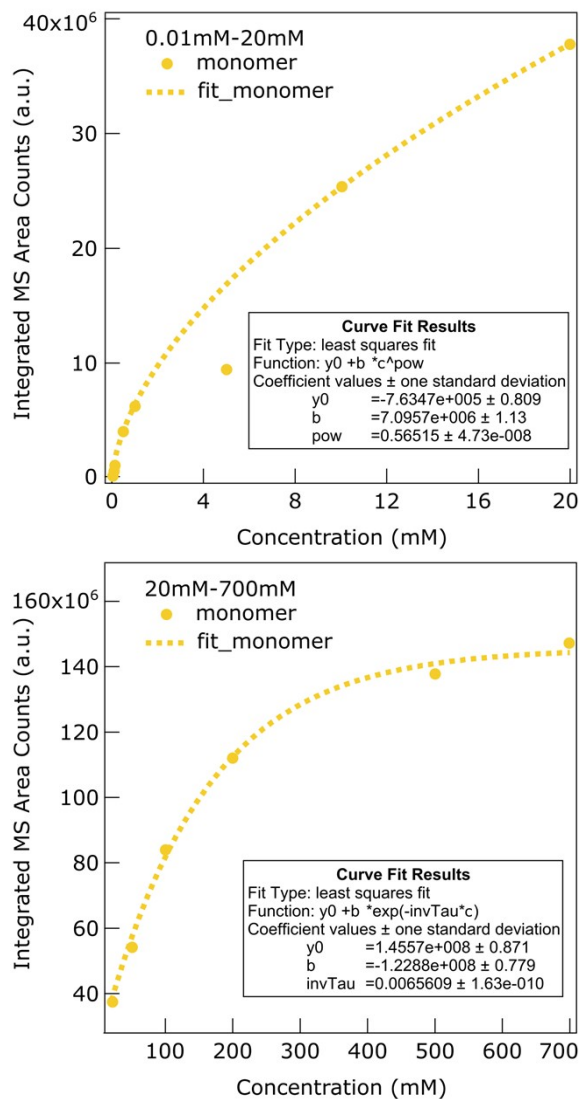
$$A(c)/F = y_0 + b \cdot e^{-\frac{c}{\tau}},$$

with the fit parameters $y_0 = 145570000$, $b = 122880000$, $\tau = 152 \text{ mM}$ determined by least square fitting and the correction factor F .

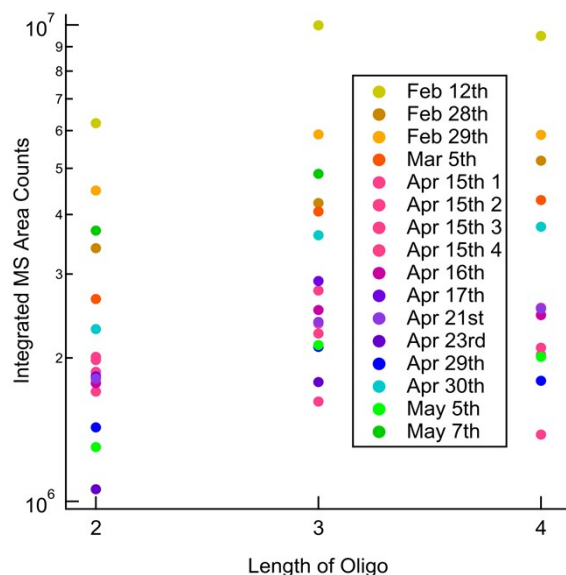
By inverting the equation, we obtain

$$c(A) = 152 \text{ mM} \cdot \ln \left(\frac{122880000}{145570000 - \frac{A}{F}} \right)$$

The decision of which of the two fit functions to use was made by comparing the peak area in question to the area of the 20 mM-standard of a measurement day: peak areas with an area greater or equal to that of the measurement day's 20 mM-standard were inserted into the exponential fit-function, below that into the power-law function. All integrated peak areas of the monomer accumulation experiments were calibrated to concentrations using the procedure described above.



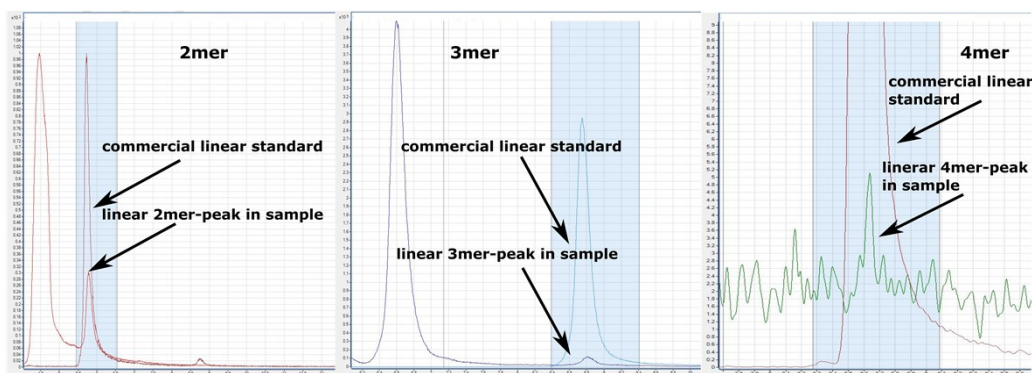
SI-FIG. S6. Fitting of monomer calibration measurement data. Mass spectrometric data from dAMP monomer measurements of known concentration (0.01 mM, 0.05 mM, 0.1 mM, 0.5 mM, 1 mM, 5 mM, 10 mM, 20 mM, 50 mM, 100 mM, 200 mM, 500 mM, 700 mM in 100 mM MOPS at pH 6.5) were extracted and integrated using the same method as for the samples. Concentration vs. peak area data points (circles) were fitted (dashed line) by least square fitting. Due to the wide range of measured concentration, the fit was performed for two intervals (0.01-20mM and 20-700mM monomer concentration) using a power-law function and an exponential function, respectively. The fit parameters determined by least square fitting are given in the box insets and in SI-Section V.1.



SI-FIG. S7. Differences in integrated MS peak area for the same oligomer concentration injection. 20 μ M of dAMP 2-4mer oligomer standards in water have been injected to the HPLC-MS on different days and months of a year. One sees a significant difference in the integrated peak area counts for different measurement days, which makes the daily correction factor F necessary.

2. AlmpdA Polymerization

In the AlmpdA polymerization, two of the possible products – the pyrophosphate and linear oligomers – had the same masses and therefore their peaks appeared in the same chromatogram. The linear oligomer was identified by comparing the retention times of the peaks with the commercially available linear oligomer standards (see SI-Fig. S8, 2mers-4mers dA-oligomers with a 5'-phosphate, 3'-dA...dA-5'P, biomers.net GmbH, with HPLC purification). The pyrophosphate oligomer peaks corresponded to those peaks that came down before the linear peaks in the same mass chromatogram following the example of [2] and [3]. To ensure that the pyrophosphate peaks were correctly identified, we performed an enzyme digestion protocol using a pyrophosphatase (see SI-Fig. S1, SI-Table S1 and SI-Section I.5). The activated oligomers had a different mass and were therefore seen individually in a different chromatogram and their peaks were easily identified. We additionally verified that the selected peaks corresponded to the correct molecule by checking the isotope distribution signature of the peak in the first charge state (see SI Chapter VI.5 for the isotope distributions).



SI-FIG. S8. Identification of the linear oligomer peaks by comparison with standards. Commercially available 3'-dA...dA-5'P oligomer standards (2-4mers) were measured and extracted using the same method as the sample (here exemplarily the 300 mM AlmpdA polymerization reaction). The linear oligomer is the one that has the same retention-peak time as the commercially available linear oligomer standard for each length.

The masses of the AlmpdA polymerization products (see SI-section VI.2) were extracted in the MassHunter Qualitative Analysis and the different charge states for each product were added up. The selected peaks from these ion count vs. time chromatograms were integrated manually using the MassHunter Qualitative Analysis program. To remove the baseline noise, we performed a background subtraction. For that, an injection of RNase-free water was measured along with the samples. Then, the oligomer masses were also extracted from the water injection as described above and their chromatograms were integrated in the same time intervals as the oligomer peaks of the samples. The resulting integration value was subtracted as background from the integrated area values of the corresponding sample peaks.

To obtain the concentration information from the integrated peak areas of the oligomers, we used a similar calibration method as for the dAMP monomers: mass spectrometric data of oligomers (2-4mers dA-oligomers) of known concentration (0.01 μM , 0.05 μM , 0.1 μM , 0.5 μM , 1 μM , 5 μM , 10 μM , 20 μM , 50 μM , 100 μM , 200 μM , 500 μM , 750 μM , 1000 μM in water) was measured and extracted with the same method as the samples. The integrated peak areas increased with increasing concentration. Concentration vs. peak area data points were fitted individually for each oligomer length using a power-law function and least square fitting. Due to the wide range of the concentrations, the least square fit was performed for two intervals: 0.01 μM -20 μM oligomer concentration and 20 μM -1000 μM with both times a power-law function but a different parameter set (see SI-Fig. S9):

$$c(A) = y_0 + b \cdot \left(\frac{A}{F}\right)^{pow}$$

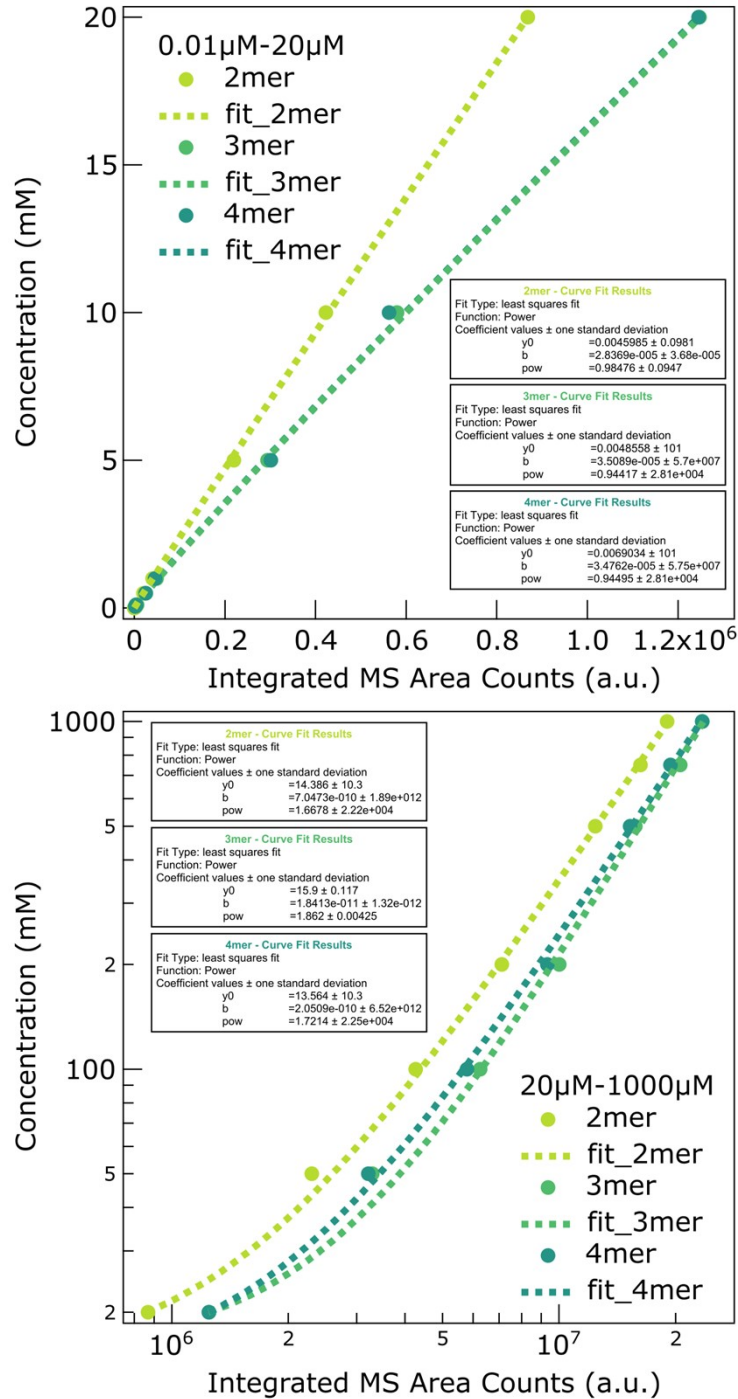
where

- A is the area of the integrated peak and $c(A)$ the concentration of the oligomer related to this peak on the day of the measurement,
- F is the factor for the daily correction and
- y_0 , b and pow are fitting parameters.

The fitting parameters for each concentration range and length of oligomer are summarized in the SI-Table S2. All integrated peak areas for the AlmpdA products were calibrated to concentrations using the procedure described above.

Length	Fit Range	$y_0(\mu\text{M})$	$b(\mu\text{M})$	pow	$A_{20\mu\text{M}Std}^{Calib}$
2mers	0.01-20 μM	4.5985e-3	2.8369e-5	0.98476	834081
	20-1000 μM	14.38	7.0473e-10	1.6678	834081
3mers	0.01-20 μM	4.8558e-3	3.5089e-5	0.94417	1102110
	20-1000 μM	15.9	1.8413e-11	1.862	1102110
4mers	0.01-20 μM	6.9034e-3	3.4762e-5	0.94495	1272060
	20-1000 μM	13.564	2.0509e-10	1.7214	1272060

SI-TAB. S2. Fitting parameters for concentration calibration measurements for the AlmpdA polymerization products. Due to the wide range of measured concentration, the least square fit was performed for two intervals (0.01 μM -20 μM and 20 μM -1000 μM oligomer concentration) by least square fitting, using different power-law functions for each interval and oligomer length.



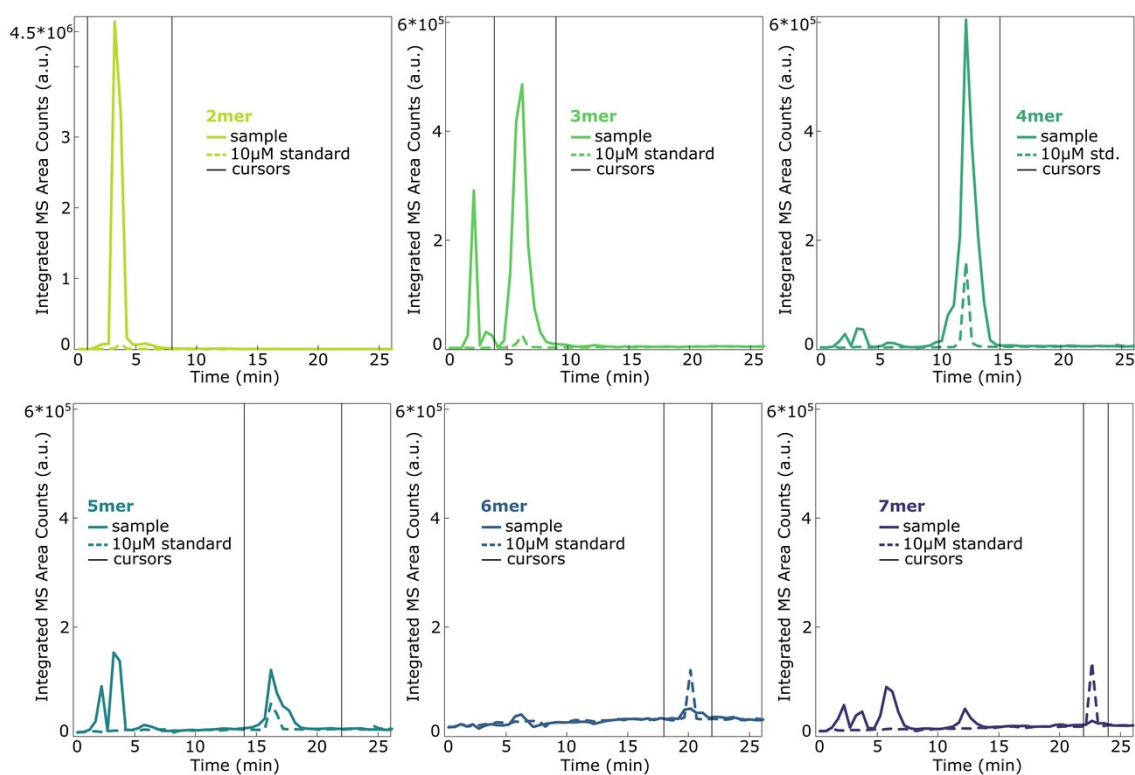
SI-FIG. S9. Fitting of dA-oligomer calibration measurement data.

Mass spectrometric data of 3'-dA...dA-5'P oligomer measurements with known concentration (0.01 μM, 0.05 μM, 0.1 μM, 0.5 μM, 1 μM, 5 μM, 10 μM, 20 μM, 50 μM, 100 μM, 200 μM, 500 μM, 750 μM, 1000 μM in water) were extracted and integrated with the same method as the samples. The concentration vs. peak area data points (dots) were fitted (dashed lines) individually for each oligomer length (2mers yellow-green, 3mers light green, 4mers dark green) by least square fitting. Due to the wide range of measured concentration, the fit was performed for two intervals (0.01 μM-20 μM and 20-700 μM monomer concentration) using a power-law function with two different sets of fit-parameters (see SI-Table S2) determined by least square fitting.

3. 2'3'cyclic Monomer Polymerization

For the quantification of polymerization products from 2'3'cyclic monomers, we used the Agilent software MassHunter Qualitative Analysis and a self-coded LabVIEW program to integrate the product chromatogram peaks. The oligomers formed during the polymerization process of 2'3'cyclic monomers had either an open 2' or 3'phosphate end or a closed 2'3'phosphate ring. The masses of these two types of polymerization products were calculated using a self-coded LabVIEW code (Dataset S1, MassListGenerato-v3.0.1lb) to the fourth charge state (see SI-section VI.3 for the resulting mass list). For mass spectrometry analysis, it was necessary to search for both types of oligomers as they differ in weight by one water molecule. Both oligomer types were extracted in single chromatograms for each length and the peaks were integrated and calibrated to concentration one by one. We extracted these m/z values from the full MS-spectra into an ion counts vs. time chromatogram using MassHunter software, allowing for an imprecision of $\Delta m/z = 2$ ppm. We saved the chromatograms as .csv ASCII files for further analysis with the LabVIEW program which is provided in Dataset S3 (TOF-Integrator2.4.1lb).

The .csv files were loaded into the LabVIEW program, which summed the chromatograms for different charged states for each possible polymerization product. For integration, the peak selection for the oligomers with an open phosphate ring was performed by comparison to commercially available standards of matching oligomer lengths (see SI-Fig. S10, 2mers-8mers G-oligomers with a 3'-phosphate, 3'-G...G-5'P, biomers.net GmbH, with HPLC purification).



SI-FIG. S10. Identification of the linear oligomer peaks by comparison with standards. Commercially available 3'P-G...G-5' oligomer standards (2-7mers) were measured and extracted using the same method as for the sample (here exemplarily a 10 mM 2'3'GMP 50 mM 2'3'CMP polymerization reaction). The linear oligomer peak was the one that had the same retention time as the commercially available linear oligomer standard for each length.

This control sample with known concentration (10 μ M per Nmer) was always measured alongside the samples from the experiment and also served for the concentration calibration later on. The peak selection for the oligomers with a closed phosphate ring was done by selecting the peak with matching mass that came down immediately before the peak of the corresponding

oligomer with the open phosphate ring of the same length. This identification was conducted with hydrolysis experiments described in [1]. The identification after the selection by mass is confirmed by checking the isotope pattern of each oligomer with a self-coded LabVIEW program provided in Dataset S3 (SpectraBrowser1.03.llb) based on the open source code “IsoSpec2: Ultrafast Fine Structure Calculator” [4]. In the program the theoretical isotope patterns (green) were compared with the measured ones (white) and only chromatograms were used for integration and quantification that showed a quality factor above 2. A closer description of the LabVIEW software can be found in [1]. All isotope patterns are documented and can be checked in Dataset S4.

The selected peaks were integrated in a time interval defined by two cursors set manually to meet the criteria described above. To remove the baseline noise, we performed a background subtraction from the integrated peak area. Depending on the type of the peak, the background subtraction was carried out either by linear extrapolation of a slanted baseline between the two cursor positions (for 3-7mers) or using the chromatogram value at the left cursor position (for 2mers) as the baseline.

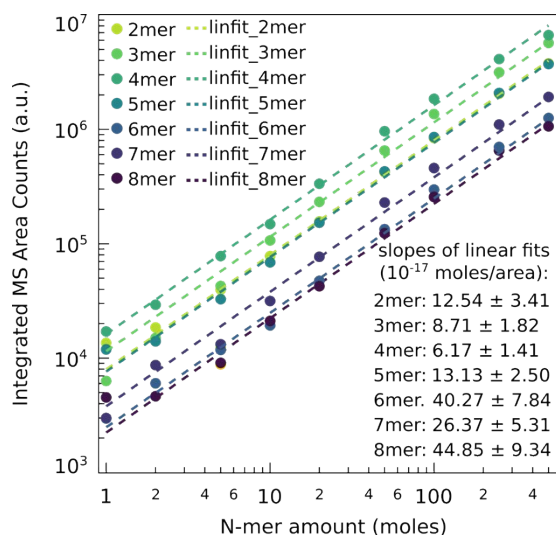
The integrated peak areas were calibrated daily with a one-point calibration using the 10 μ M-standards to obtain the concentration values of the oligomers from the HPLC-MS measurements. We used a one-point-calibration because we showed that the oligomer amount (in moles) scaled linearly with the integrated peak area (see SI-Fig S11).

Thus, we calculated the concentration of an oligomer of a certain length n in a sample under study c_{smp}^n from the following quantities:

- c_{Std}^n : concentration of oligomers of length n in the injected standard
- A_{Std}^n : integrated peak area of an oligomer of length n in the injected standard
- A_{smp}^n : integrated peak area of an oligomer of length n in the injected sample
- V_{smp} : injection volume of the sample
- V_{Std} : injection volume of the standard

$$c_{smp}^n = (A_{smp}^n * (c_{Std}^n * V_{Std}) / A_{Std}^n) / V_{smp}.$$

In this way, we calculated the concentration of each oligomer of each length and ending type (closed or open) in the samples.



SI-FIG. S11. The oligomer amount (in moles) scales linearly with the integrated peak area. Commercially available 2-8mer polyG oligomers (3’P-G...G-5’, 3’-phosphate biomers.net GmbH, with HPLC purification) with known amounts (1 pmol, 2 pmol, 5 pmol, 10 pmol, 20 pmol, 50 pmol, 100 pmol, 250 pmol, 500 pmol in water) were measured, extracted and integrated with the same method as the RNA polymerization samples.

In search for a fit function for the area to moles relationship, we found that the data points (dots) for oligomer amount (in moles) to integrated peak area were best fitted with linear functions for all oligomers lengths (dashed lines).

VI. MASS LISTS AND CHEMICAL FORMULAS

For the experiments for Figures 1 and 2, the masses were calculated to the fourth decimal using the Agilent Isotope Distribution Calculator. We report the masses of the full isotopic distribution for the first charge state; for the other charge states, we give only the most abundant isotope.

For the experiments for Figure 3, the masses were calculated using a self-coded LabVIEW program (Dataset S6, Kinetics_ADp_polymerization_7.0.llb). We report the masses of the most abundant isotope for all calculated charge states.

1. dAMP

dAMP: $C_{10}H_{14}O_6N_5P$

m/z (u)	Charge State	Abundance (%)
331.0682	0H	100
330.0609	-1H	100
331.0634	-1H	13.02
332.0654	-1H	2.02
333.0677	-1H	0.19
333.0677	-1H	0.02

2. AlmpdA Polymerization

Linear and Pyrophosphate Oligomer Masses:

5'P-AA-3': $C_{20}H_{26}O_{11}N_{10}P_2$

m/z (u)	Charge State	Abundance (%)
644.1258	0H	100
643.1185	-1H	100
644.1210	-1H	25.99
645.1232	-1H	5.51
646.1255	-1H	0.85
647.1277	-1H	0.11
648.1299	-1H	0.01

5'P-AAA-3': $C_{30}H_{38}O_{16}N_{15}P_3$

m/z (u)	Charge State	Abundance (%)
957.1834	0H	100
956.1761	-1H	100
957.1786	-1H	38.96

958.1809	-1H	10.69
959.1832	-1H	2.19
960.1854	-1H	0.38
961.1876	-1H	0.06
962.1898	-1H	0.01
477.5844	-2H	100

5'P-AAAA-3': C₄₀H₅₀O₂₁N₂₀P₄

m/z (u)	Charge State	Abundance (%)
1270.2410	0H	100
1269.2337	-1H	100
1270.2362	-1H	51.93
1271.2385	-1H	17.55
1272.2408	-1H	4.45
1273.2431	-1H	0.93
1274.2453	-1H	0.17
1275.2476	-1H	0.03
634.1132	-2H	100
422.4064	-3H	100

Cyclic Oligomer Masses:

Chemical Formula	m/z (u)	Charge State	Abundance (%)
C ₂₀ H ₂₄ O ₁₀ N ₁₀ P ₂	625.1079	-1H	100
(Dimer)	312.0503	-2H	100
C ₃₀ H ₃₆ O ₁₅ N ₁₅ P ₃	938.1655	-1H	100
(Trimer)	468.5791	-2H	100
	312.0503	-3H	100
C ₄₀ H ₄₈ O ₂₀ N ₂₀ P ₄	1251.2231	-1H	100
(Tetramer)	625.1079	-2H	100
	416.4029	-3H	100
	312.0503	-4H	100

Activated Oligomer Masses:

Chemical Formula	m/z (u)	Charge State	Abundance (%)
C ₁₃ H ₁₇ O ₅ N ₈ P (Monomer)	395.0987	-1H	100

C ₂₃ H ₂₉ O ₁₀ N ₁₃ P ₂	708.1563	-1H	100
(Dimer)	353.5745	-2H	100
C ₃₃ H ₄₁ O ₁₅ N ₁₈ P ₃	1021.2139	-1H	100
(Trimer)	510.1033	-2H	100
	339.7331	-3H	100
C ₄₃ H ₅₃ O ₂₀ N ₂₃ P ₄	1334.2715	-1H	100
(Tetramer)	666.6321	-2H	100
	444.0856	-3H	100

3. 2'3'cyclic Monomer Polymerization

Masses for Oligomers with Open Phosphate Ring:			Masses for Oligomers with Closed Phosphate Ring:		
Base Composition	m/z (u)	Charge State	Base Composition	m/z (u)	Charge State
GG	707.0981	-1H	GG	689.0876	-1H
GC	667.092	-1H	GC	649.0814	-1H
CC	627.0859	-1H	CC	609.0753	-1H
GGG	1052.146	-1H	GGG	1034.135	-1H
GGC	1012.139	-1H	GGC	994.1289	-1H
GCC	972.1333	-1H	GCC	954.1227	-1H
CCC	932.1271	-1H	CCC	914.1166	-1H
GGGG	1397.193	-1H	GGGG	1379.183	-1H
	698.0929	-2H		689.0876	-2H
GGGC	1357.187	-1H	GGGC	1339.176	-1H
	678.0898	-2H		669.0845	-2H
GGCC	1317.181	-1H	GGCC	1299.17	-1H
	658.0867	-2H		649.0814	-2H
GCCC	1277.175	-1H	GCCC	1259.164	-1H
	638.0836	-2H		629.0784	-2H
CCCC	1237.168	-1H	CCCC	1219.158	-1H
	618.0806	-2H		609.0753	-2H
GGGGG	1743.244	-1H	GGGGG	1725.233	-1H
	871.1183	-2H		862.113	-2H
	580.4097	-3H		574.4062	-3H
GGGGC	1703.238	-1H	GGGGC	1685.227	-1H
	851.1152	-2H		842.1099	-2H

	567.0744	-3H		561.0708	-3H
GGGCC	1663.232	-1H	GGGCC	1645.221	-1H
	831.1121	-2H		822.1068	-2H
	553.739	-3H	GGCCC	1605.215	-1H
GGCCC	1623.225	-1H		802.1038	-2H
	811.109	-2H	GCCCC	1564.205	-1H
GCCCC	1582.216	-1H		781.599	-2H
	790.6043	-2H	CCCCC	1524.199	-1H
CCCCC	1542.21	-1H		761.5959	-2H
	770.6012	-2H	GGGGGG	2070.281	-1H
GGGGGG	2088.291	-1H		1034.637	-2H
	1043.642	-2H		689.422	-3H
GGGGGC	2048.285	-1H	GGGGGC	2030.275	-1H
	1023.639	-2H		1014.634	-2H
	682.0902	-3H		676.0867	-3H
GGGGCC	2008.279	-1H	GGGGCC	1990.268	-1H
	1003.636	-2H		994.6305	-2H
	668.7548	-3H		662.7513	-3H
GGGCCC	1968.273	-1H	GGGCCC	1950.262	-1H
	983.6328	-2H		974.6275	-2H
	655.4194	-3H		649.4159	-3H
GGCCCC	1928.267	-1H	GGCCCC	1910.256	-1H
	963.6297	-2H		954.6244	-2H
	642.084	-3H		636.0805	-3H
GCCCCC	1888.261	-1H	GCCCCC	1870.25	-1H
	943.6266	-2H		934.6213	-2H
	628.7486	-3H		622.7451	-3H
CCCCCC	1848.254	-1H	CCCCCC	1830.244	-1H
	923.6235	-2H		914.6182	-2H
	615.4133	-3H		609.4097	-3H
GGGGGGG	2433.339	-1H	GGGGGGG	2415.328	-1H
	1216.166	-2H		1207.16	-2H
	810.4414	-3H		804.4378	-3H
	607.5792	-4H		603.0766	-4H
GGGGGGC	2393.333	-1H	GGGGGGC	2375.322	-1H
	1196.163	-2H		1187.157	-2H
	797.106	-3H		791.1025	-3H

	597.5777	-4H		593.075	-4H
GGGGGCC	2353.326	-1H	GGGGGCC	2335.316	-1H
	1176.16	-2H		1167.154	-2H
	783.7706	-3H		777.7671	-3H
	587.5761	-4H		583.0735	-4H
GGGGCCC	2313.32	-1H	GGGGCCC	2295.31	-1H
	1156.157	-2H		1147.151	-2H
	770.4352	-3H		764.4317	-3H
	577.5746	-4H		573.072	-4H
GGGCCCC	2273.314	-1H	GGGCCCC	2255.304	-1H
	1136.153	-2H		1127.148	-2H
	757.0998	-3H		751.0963	-3H
	567.5731	-4H		563.0704	-4H
GGCCCCC	2233.308	-1H	GGCCCCC	2215.297	-1H
	1116.15	-2H		1107.145	-2H
	743.7645	-3H		737.7609	-3H
	557.5715	-4H		553.0689	-4H
GCCCCCC	2193.302	-1H	GCCCCCC	2175.291	-1H
	1096.147	-2H		1087.142	-2H
	730.4291	-3H		724.4255	-3H
CCCCCCC	2153.296	-1H	CCCCCCC	2135.285	-1H
	1076.144	-2H		1067.139	-2H
	717.0937	-3H		711.0902	-3H

VIII. ERROR ESTIMATIONS

1. Figure 3

The experiments for Fig. 3 were repeated three times with the same parameters (except for the pore experiment of G/C ratio 1mM/5mM which was repeated twice). The experimental results were averaged and the mean values were plotted in the graphs. The error bars of the data points are the standard deviations of the mean of triplicates (or of the duplicate for the pore experiments of G/C ratio 1mM/5mM).

2. Figures 1 and 2

For estimating the errors of the experiments shown in Figures 1 and 2, we averaged the relative errors for all datapoints of the experiments in Figure 3 from the standard deviations of the mean of replication experiments as explained in the paragraph before. This allowed us to get an estimate of a generalized error introduced by thermal pore experiments and measurements by HPLC/ESI-

TOF. These errors in average amount to 47.5%, which made us assume an error of +/- 50% to the base for all datapoints in Fig.1 and 2.

IX. FINITE ELEMENT SIMULATION OF ACCUMULATION AND POYLMERIZATION IN A THERMOPHORETIC PORE

In order to investigate the effect of thermal non-equilibria, i.e. temperature gradients due to heat flows on a system, we used a 2-dimensional finite element simulation (COMSOL Multiphysics 5.4). There we simulated the heat transfer, the convection of the bulk liquid, and the transport of the diluted species in the thermal gradient of our pores.

The full chamber model used for the experiments was recreated using 3D CAD software and imported into the finite element software (SI-Fig. S12a). Thermal conductivities were taken from the Comsol internal database or from the product data sheets of the materials used and are $k_{H_2O} = 0.62 \text{ W/mK}$ for water, $k_{Steel} = 44.5 \text{ W/mK}$ for the steel frames, $k_{Alu} = 237 \text{ W/mK}$ for the aluminium elements, $k_{Sapphire} = 35 \text{ W/mK}$ for the sapphire elements and $k_{FEP} = 0.2 \text{ W/mK}$ the FEP-Teflon foil.

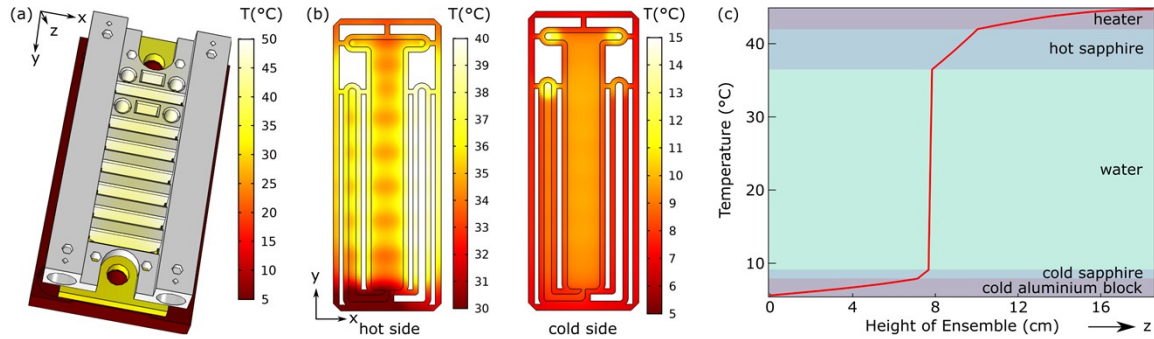
Since the space around the actual water-filled pocket is fully covered by Teflon, an insulating thermal boundary condition for the heat flow through the outer surfaces of the COMSOL model was assumed, i.e. $q_{extSurface} = 0$. The heat conduction was then calculated according to SI-Equation (1)

$$\rho c_p \left(\frac{\partial T}{\partial t} + \mathbf{u} * \nabla T \right) + \nabla(k \nabla T) = q \quad (1)$$

and solved for the entire structure, where ρ is the density, c_p the specific heat capacity and k the thermal conductivity of the respective material, T the temperature, q the heat flow and \mathbf{u} the velocity vector of the solution in the chamber. In the stationary case and assuming a very slow fluid velocity \mathbf{u} due to the small dimensions of the pore and the resulting strong laminarity of the liquid flows, SI-Eq. (1) simplifies to

$$\nabla T * (k \nabla T) = q \quad (2)$$

whose solution is shown in SI-Fig. S12.



SI-Fig. S12 Geometric Model in the Finite Element Simulation and Heat Conduction Simulation. (a) The full three-dimensional model including all elements shown in SI-Fig. S2 with color coding for the simulated temperatures (in °C). (b) It was important that the temperature distribution in the x-y-plane was as uniform as possible. Along the z-axis, i.e. in the direction of the heat flow vertically through the thin water layer, the temperature drop should be as linear as possible. Also we needed optical observation of the sample in the heat flow cell. This was achieved by the combination of a 2 mm thick sapphire on the hot chamber side, which compensates for thermal unevenness due to the viewing windows in the slit aluminum heater (see SI-Fig. S2). The two-dimensional temperature plot in the x-y-plane depicts the calculated temperature distribution on the x-y surface on the hot and the cold side of the water-filled pore, showing that the temperature distribution is homogeneous in the x-y-plane with maximum deviations of about 2°C on the hot side of the solution and less

than 0.5°C on the cold side of the solution. (c) One-dimensional temperature plot along the z-axis of the whole model. Most of the temperature difference falls off in the 170 μm thick microfluidic chamber filled with aqueous solution (around 70% of the entire temperature drop).

The resulting temperature distribution within the fluid was then coupled to the Navier-Stokes equation via the temperature dependent density $\rho(T)$ and viscosity $\eta(T)$

$$\rho(T)(u\nabla)u = \nabla \left[-p + \eta(\nabla u + (\nabla u)^\top) - \frac{2}{3}\eta(\nabla u) \right] - e_y g \rho(T) \quad (3)$$

where \mathbf{u} is the velocity vector of the fluid, p is the local pressure, e_y is the unit vector in y-direction and g is the gravitational acceleration. After setting a non-slip boundary condition at all surfaces, a complete numerical solution for \mathbf{u} could be found.

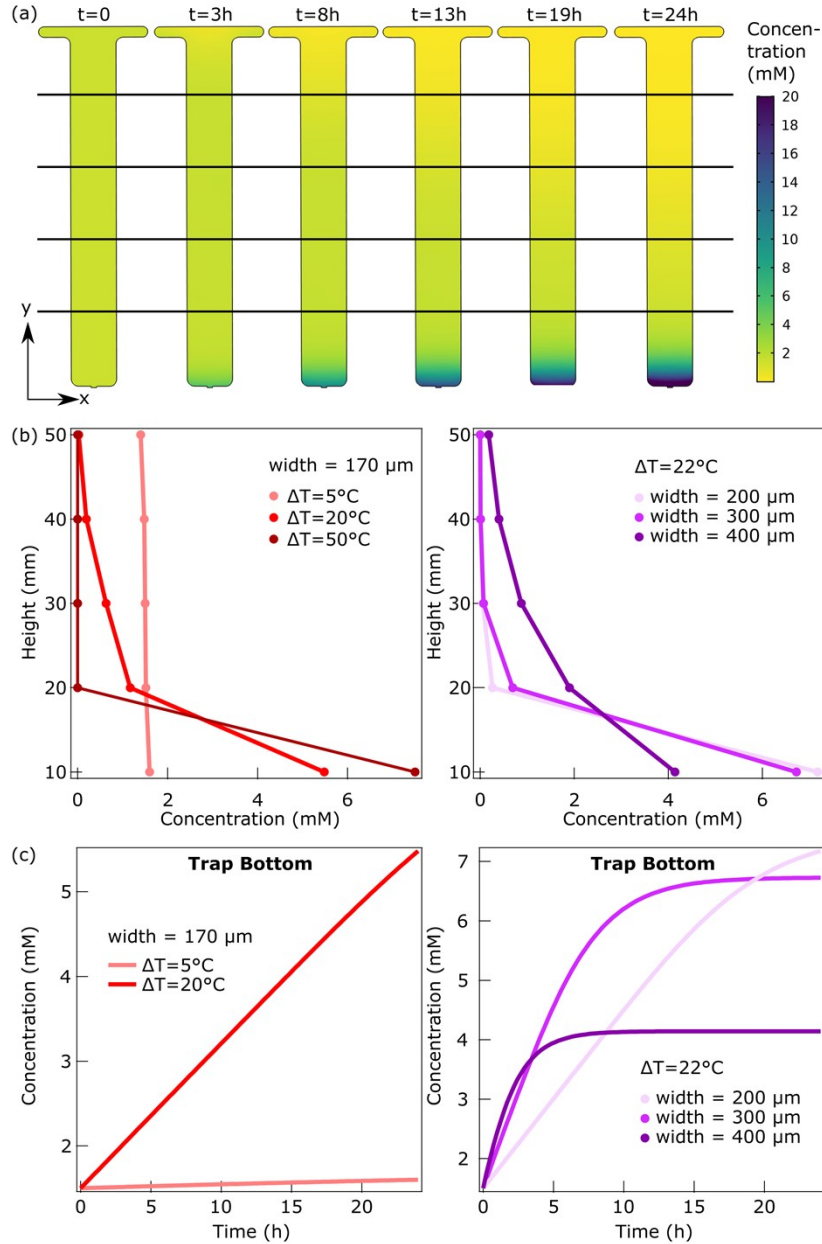
To determine the concentration of the dAMP monomers in the pore, the numerical model was further extended by a drift-diffusion component. This includes thermophoresis, *i.e.* the movement of the dissolved molecule along the temperature difference, normal diffusion, which counteracts local concentration gradients and the coupling to the velocity field of the solution:

$$\nabla(-D\nabla c + (u + S_T D \nabla T) c) = 0, \quad (4)$$

where D is the normal diffusion coefficient, c the local concentration and S_T the Soret coefficient of the dAMP monomers. The coupling of SI-Eq. (4) to SI-Eqs. (2) and (3) is achieved by the temperature T and the velocity field \mathbf{u} . The solutions to SI-Eq. (4) give the concentration results in Figs. 1-4 in the main text.

1. Robustness of Accumulation

To map out the effect of different temperature gradients and different pore widths on a monomer accumulation we swept parameters over a broad range of pore conditions: $\Delta T = 5 - 50^\circ\text{C}$ and $w = 100 \mu\text{m} - 400 \mu\text{m}$. The results are shown in SI-Fig. S13. The values for theoretical monomers of $D = 643 \mu\text{m}^2/\text{s}$ and $S_T = 0.001 \frac{1}{\text{K}}$ were taken from [3]. The Comsol file of the simulation is provided in Dataset S5.



SI-FIG. S13. Coupled Solution of Heat Conduction, Navier-Stokes Flow and Thermal Drift Diffusion of the dAMP Monomers Under Different Parameters. (a) Simulated concentration distribution of dAMP monomers (1.5 mM starting concentration) in the x-y-plane of a pore after 24 h of accumulation with $\Delta T = 22^\circ\text{C}$ and pore width $w = 170\ \mu\text{m}$. For arriving at the simulated concentration values that are displayed for each height value in (b), an integration within the depicted x-y-regions had to be performed (black lines). (b) Concentration distribution along the height of a simulated pore of 1.5 mM dAMP monomers after 24 h with $w = 170\ \mu\text{m}$ and $\Delta T = 5^\circ\text{C}$ (light red), $\Delta T = 20^\circ\text{C}$ (red) and $\Delta T = 50^\circ\text{C}$ (dark red) as well as with $\Delta T = 22^\circ\text{C}$ and $w = 200\ \mu\text{m}$ (light purple), $w = 300\ \mu\text{m}$ (purple) and $w = 400\ \mu\text{m}$ (dark purple). Steeper temperature gradients and thinner widths led to a stronger accumulation along the height of the pore due to the quicker convection flow and stronger thermophoresis. (c) Simulated concentration evolution at the bottom stripe of a pore over time with 1.5 mM dAMP monomer starting concentration with $w = 170\ \mu\text{m}$ and $\Delta T = 5^\circ\text{C}$ (light red), $\Delta T = 20^\circ\text{C}$ (red) and $\Delta T = 50^\circ\text{C}$ (dark red) as well as with $\Delta T = 22^\circ\text{C}$ and $w = 200\ \mu\text{m}$ (light purple), $w = 300\ \mu\text{m}$ (purple) and $w = 400\ \mu\text{m}$ (dark purple). A steeper temperature gradient led to a quicker and stronger accumulation and a smaller pore width led to an later reaching of the steady stated however a higher concentration at the bottom.

2. dAMP Accumulation

The solutions for SI-Eq. (4) for pure monomer accumulation (with out any chemical reactions) for the three different starting concentration 300 mM, 20 mM and 2.5 mM are shown in Fig. 1c in the main text. The parameters obtained by fitting the experimental results are shown in SI-Table S3. The parameter set optimizes the fit for all three different starting concentrations, showing their universality. The Comsol file of the simulation are provided in Dataset S5.

Parameter	Value	Explanation
Pore Width	170 μm	width of pore
Pore Height	43.5 mm	height of pore
T_{cold}	8°C	temperature on cold side of pore
ΔT	25 K	temperature gradient between hot and cold side of pore (fit-parameter)
n	0.2	fit-parameter for molecule properties (fit-parameter)
D	$643 \cdot n^{-0.46} \mu\text{m}^2/\text{s}$	formula for diffusion coefficient of molecules
S_T	$(5.3 + 5.7 \cdot n^{0.73}) \cdot 10^{-3} 1/\text{K}$	formula for Soret coefficient of molecules
A1L	2.5 mM	initial monomer concentration of 2.5mM experiments
A1M	20 mM	initial monomer concentration of 20 mM experiments
A1H	300 mM	initial monomer concentration of 300 mM experiments

SI-TAB. S3. Simulation Parameters for Monomer Accumulation in a Thermogravitational Pore The same parameter set could be used to model all three starting concentrations of the monomer accumulation experiments in a thermophoretic pore.

3. AlmpdA Accumulation and Polymerization

To simulate the combined accumulation and polymerization of the AlmpdA strand formation reaction in a thermal pore the SI-Eq. (4) was calculated for all oligolengths and types that were detected in the experiment (active: 2-4nt, linear: 2-4nt, pyrophosphate: 2-4nt) and were coupled by the following rate equations:

Activated Monomer (A1):	$\begin{aligned} d(A1)/dt = & -op \cdot A1 - 4 \cdot on \cdot A1 \cdot A1 - 2 \cdot on \cdot A1 \cdot A2 - 2 \cdot on \cdot A1 \cdot A3 \\ & - 1 \cdot on \cdot A1 \cdot L1 - 1 \cdot on \cdot A1 \cdot L2 - 1 \cdot on \cdot A1 \cdot L3 \\ & - 2 \cdot onp \cdot A1 \cdot A1 - 1 \cdot onp \cdot A1 \cdot A2 - 1 \cdot onp \cdot A1 \cdot A3 \\ & - 1 \cdot on \cdot A1 \cdot P2 - 1 \cdot on \cdot A1 \cdot P3 \end{aligned}$
Activated Dimer (A2):	$\begin{aligned} d(A2)/dt = & -op \cdot A2 - 2 \cdot on \cdot A2 \cdot A1 - 4 \cdot on \cdot A2 \cdot A2 + 2 \cdot on \cdot A1 \cdot A1 \\ & - 1 \cdot on \cdot A2 \cdot L1 - 1 \cdot on \cdot A2 \cdot L2 - 1 \cdot onp \cdot A2 \cdot A1 \\ & - 2 \cdot onp \cdot A2 \cdot A2 - 1 \cdot on \cdot A2 \cdot P2 \end{aligned}$
Activated Trimer (A3):	$\begin{aligned} d(A3)/dt = & -op \cdot A3 - 2 \cdot on \cdot A3 \cdot A1 + 2 \cdot on \cdot A1 \cdot A2 - 1 \cdot on \cdot A3 \cdot L1 \\ & - 1 \cdot onp \cdot A3 \cdot A1 \end{aligned}$
Activated Tetramer (A4):	$d(A4)/dt = -op \cdot A4 + 2 \cdot on \cdot A1 \cdot A3 + 2 \cdot on \cdot A2 \cdot A2$
Linear Monomer (L1):	$\begin{aligned} d(L1)/dt = & +op \cdot A1 - 1 \cdot on \cdot L1 \cdot A1 - 1 \cdot on \cdot L1 \cdot A2 - 1 \cdot on \cdot L1 \cdot A3 \\ & - 1 \cdot onp \cdot A1 \cdot L1 - 1 \cdot onp \cdot A2 \cdot L1 - 1 \cdot onp \cdot A3 \cdot L1 \end{aligned}$
Linear Dimer (L2):	$d(L2)/dt = +op \cdot A2 + 1 \cdot on \cdot A1 \cdot L1 - 1 \cdot on \cdot L2 \cdot A1 - 1 \cdot on \cdot L2 \cdot A2$

	$-1*on_p*A1*L2 -1*on_p*A2*L2$
Linear Trimer (L3):	$d(L3)/dt = +op*A3 +1*on*A1*L2 +1*on*A2*L1 -1*on*L3*A1 -1*on_p*A1*L3$
Linear Tetramer (L4):	$d(L4)/dt = +op*A4 +1*on*A1*L3 +1*on*A3*L1 +1*on*A2*L2$
Pyrophosphate Dimer (P2):	$d(P2)/dt = +1*on_p*A1*A1 -1*on*P2*A1 -1*on*P2*A2$
Pyrophosphate Trimer (P3):	$d(P3)/dt = +1*on_p*A1*A2 +1*on*A1*P2 -1*on*P3*A1$
Pyrophosphate Tetramer (P4):	$d(P4)/dt = +1*on_p*A1*A3 +1*on_p*A2*A2 +1*on*A1*P3 +1*on*A2*P2 +1*on_p*A2*L2 +1*on_p*A1*L3 +1*on_p*A3*L1$

The parameters for the simulations for all three different starting concentrations were adopted from the previously determined parameters of the pure monomer accumulation and completed by on-rates for the polymerization equations and deactivation-rates for the imidazolization and can be found in SI-Table S4. The Comsol file of the simulation is provided in Dataset S5.

Parameter	Value	Explanation
Pore Width	170 μm	width of pore
Pore Height	43.5 mm	height of pore
T_{cold}	8°C	temperature on cold side of pore
ΔT	19 K	temperature gradient between hot and cold side of pore (fit-parameter)
n	0.2	fit-parameter for molecule properties (fit-parameter)
D	$643*n^{-0.46} \mu\text{m}^2/\text{s}$	formula for diffusion coefficient of molecules
S_T	$(5.3+5.7*n^{0.73})*10^{-3} 1/\text{K}$	formula for Soret coefficient of molecules
A1small	2.5 mM	initial monomer concentration of 2.5 mM experiments
A1middle	20 mM	initial monomer concentration of 20 mM experiments
A1large	25 mM	initial monomer concentration of 300 mM experiments (fit-parameter)
op	$1.6*10^{-6} 1/\text{s}$	deactivation off-rate of imidazole activation (fit-parameter)
on	$2.5*10^{-9} 1/(\text{s}*mol/\text{m}^3)$	on-rate into active or linear oligomers (fit-parameter)
on _p	$5.6*on$	on-rate into pyrophosphate oligomers (fit-parameter)

SI-TAB. S4. Simulation Parameters for Combined AlmpdA Accumulation and Polymerization The same parameter set could be used to model all three starting concentrations of the AlmpdA polymerization and accumulation experiments in a thermophoretic pore. The starting concentration for the largest initial AlmpdA concentration was weighed in to be 300 mM but had to be modeled to 25 mM in the simulation to fit the experimental results: This is explainable by the fact, that already by eye a precipitation of the dissolved molecules took place in the pore due to the strong accumulation in the thermophoretic pore.

4. 2',3'-cyclic Accumulation and Polymerization

To simulate the combined accumulation and polymerization of the 2',3'-cyclic polymerization reaction in a thermal pore the SI-Eq. (4) was calculated for all oligolengths and base compositions that were detected in the experiment (GG, GC, CC, GGG, GGC, ... , GCCCCCC, CCCCCCC) and were coupled by the rate equations that are provided in Dataset S6. There also the self-coded LabVIEW program to get the rate equations can be found (Kinetics_ADP_polymerization_7.0.llb).

The parameters for the simulations were adopted from the previously found parameters of the pure monomer accumulation and completed by length- and sequence-dependent on-rates for the polymerization equations and a k_{off} rate for the deactivation of the 2',3'-cyclic phosphate ends to either 2' or 3' phosphate. We assumed the same rate for polymers or monomers. Parameters can be found in SI-Table S5. The Comsol file of the simulation is provided in Dataset S5.

Parameter	Value	Explanation
Pore Width	170 μm	width of pore
Pore Height	43.5 mm	height of pore
T_{cold}	40°C	temperature on cold side of pore
ΔT	30 K	temperature gradient between hot and cold side of pore (fit-parameter)
reaction-height	Pore Width	zone inside the pore in which the polymerization can take place, modelling the zone where the air-water interface in the experiment is triggering the wet-dry cycles and hence the polymerization
n	0.2	fit-parameter for molecule properties (fit-parameter)
D	$643 \cdot n^{-0.46} \mu\text{m}^2/\text{s}$	formula for diffusion coefficient of molecules
S_T	$(5.3 + 5.7 \cdot n^{0.73}) \cdot 10^{-3} \text{ 1/K}$	formula for Soret coefficient of molecules
C_{init}	50 mM	initial monomer concentration for 2',3'-cCMP monomers in the 10/50 experiments
G_{init}	10 mM	initial monomer concentration for 2',3'-cGMP monomers in the 10/50 experiments
k_{on}	$9.5 \cdot 10^{-7} \text{ 1}/(\text{s} \cdot \text{mol}/\text{m}^3)$	general on-rate for general polymerization (not monomer-to-monomer-polymerization) fit-parameter
k_{11}	$k_{\text{on}}/60$	on-rate when two monomers polymerize (fit-parameter)
k_{GG}	1	factor to modulate the on-rate when two GMPs are polymerized (fit-parameter)
k_{GC}	0.03	factor to modulate the on-rate when a GMP and a CMP are polymerized (fit-parameter)
k_{CC}	0.04	factor to modulate the on-rate when two CMPs are polymerized (fit-parameter)
k_{off}	1/day	off-rate for the opening (deactivation) of the 2',3'-cyclic phosphate end

SI-TAB. S5. Simulation Parameters for Combined 2',3'-Cyclic Polymerization and Accumulation To simulate the very peculiar hammock distribution of the base-composition in the strands emerging from the 2',3'-cyclic polymerization (see Fig. 3c in the main text) we included a lower k_{on} rate for the reaction of two monomers (k_{11}) with one another than for any other polymerization reaction between two other strand lengths and and a k_{off} rate for the deactivation of the 2',3'-cyclic phosphate ends of activated polymers and monomers. To attribute for the strong G-preference in the strand formation reaction of this chemistry we included factors

that attenuate the reaction between a G- and a C- or a C- and a second C-base nucleotide – unimportant if as a monomer or at the end of a strand.

5. Longtime Extrapolation With and Without Feeding

For the 0D simulation we could ramp up the length of simulated strands to 21nt (250 sequence-diverse species and rate equations, see Dataset S6, plotted in Fig.4a until 12nt). The “no feeding” simulation allows for the monomer concentration to diminish over time. This simulates a real pore in steady state that cannot fill up the monomers that are used up by polymerization. In the “with feeding” simulation the monomer concentrations of 2',3'-cCMP and 2',3'-cGMP are set to constant in order to simulate the refill of monomers by the open pore and permanent income of new monomers at the top of a real pore from an outer reservoir.

For the 2D simulations of the longtime monomer accumulation in Figures 4a and b, the same simulation was used as in IX.2. and was extended to the times of up to one year. For the calculation of “no feeding” all outer boundaries of the 2D pore simulation did not exchange molecules with the outside, for “with feeding”, the top boundary of the pore was set to a constant concentration of 1 μM , which simulated the connection of a real pore to a large reservoir with 1 μM monomer concentration, like for example a primordial ocean.

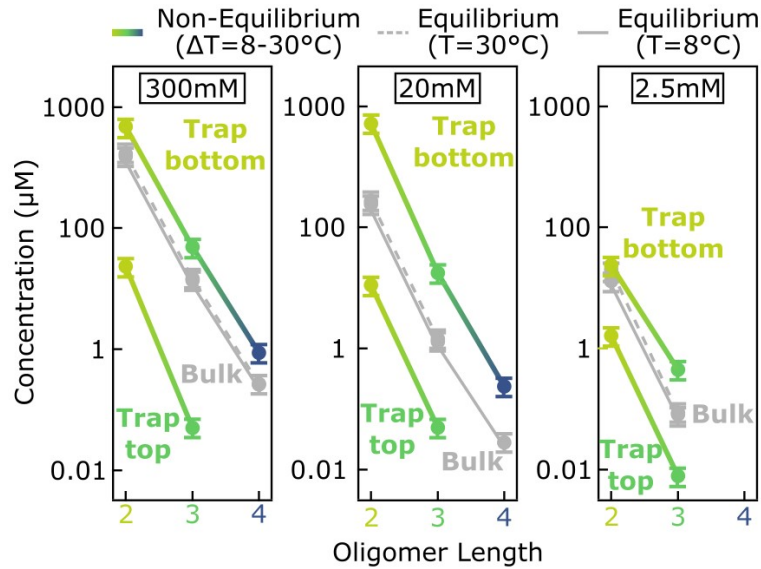
The parameters for the 0D simulations of Figure 4c and d were adopted from the 2D simulation of Fig 3c. The polymerization rate was slightly tuned to both include a hydrolysis reaction channel and still match the results of Figure 3c. The 0D simulation was fed with 0.6 $\mu\text{M/s}$ inferred from the 2D simulation of 4a. All parameters can be found in SI-Table S6. The Comsol files of both longtime simulations (pure monomer accumulation and with polymerization reaction) are provided in Dataset S5.

Parameter	Value (a.u.)	Explanation
C_{init}	50000	initial monomer concentration for 2',3'-cCMP monomers in the 10/50 experiments
G_{init}	10000	initial monomer concentration for 2',3'-cGMP monomers in the 10/50 experiments
k_{on}	$1.6 \cdot 10^{-9}$	on-rate for general polymerization (not monomer-to-monomer-polymerization), fit-parameter taken from adapting the 0D simulation to Figure 3c.
k_{11}	$k_{\text{on}}/60$	on-rate when two monomers polymerize
k_{GG}	1	factor to modulate the on-rate when two GMPs are polymerized
k_{GC}	0.03	factor to modulate the on-rate when a GMP and a CMP are polymerized
k_{CC}	0.04	factor to modulate the on-rate when two CMPs are polymerized
op	1/day	deactivation-rate for the opening (deactivation) of the 2',3'-cyclic phosphate end
ofd	1/2days or 1/90days	hydrolysis-rate of the oligomer backbone, breaking into smaller pieces with a 2' or 3' phosphate ending
feedrate	0.6/3600	feeding-rate of 0.6 $\mu\text{M/s}$ to the pore

SI-TAB. S6. Simulation Parameters for 0D Longtime 2',3'-Cyclic Polymerization With and Without Feeding The parameters for the 0D simulations were largely adopted from the previously determined parameters of the 2',3'-cyclic polymerization in 2D (see SI-Table S5) however without units due to the dimensionless 0D simulation. Feed rate and hydrolysis rate are newly added parameters.

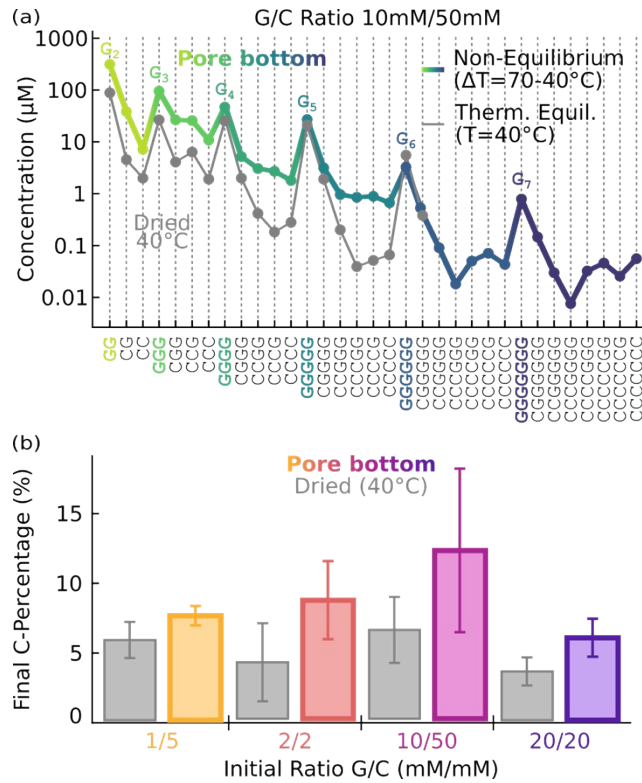
X. ADDITIONAL FIGURES

Fig. S14.



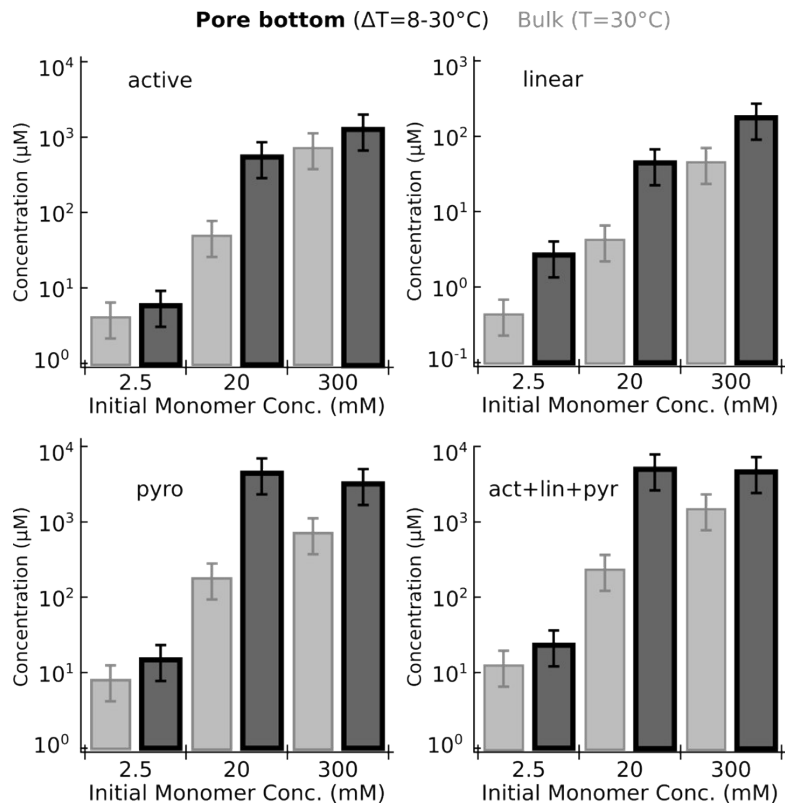
SI-FIG. S14. Accumulation in a heated rock pore enhances the polymerization of preactivated DNA monomers compared to bulk experiments in thermal equilibrium for all lengths. (a) AlmpdA monomer polymerization (see SI-section I.2) was run for 24 h in a pore ($\Delta T=30-8^{\circ}\text{C}=22^{\circ}\text{C}$) and in the bulk ($T=8^{\circ}\text{C}$ and $T=30^{\circ}\text{C}$) with starting concentrations of 300 mM, 20 mM and 2.5 mM AlmpdA monomers. After freeze extraction and analysis, we plotted the sum of polymerization products (pyrophosphate, linear and activated oligomers) for each length, and compared what we measured at the pore top, at the pore bottom (green) and in the bulk at isothermal conditions (gray). Oligomers with lengths of 2 nt (yellow-green), 3 nt (green) and 4 nt (blue) were formed for 300 mM and 20 mM starting monomer concentrations, 2mers and 3mers were formed for 2.5 mM. For all experiments, the oligomer concentration at the bottom of the pore exceeded the product concentration in bulk solution. Error bars indicate 50 % error estimates (see SI-section VIII.2). Lines are guides to the eye.

Fig. S15.



SI-FIG. S15. The Thermal Pore Enhances the Incorporation of the Disfavoured 2',3'cCMP (a) By HPLC/ESI-TOF analysis we could determine the base compositions of the oligomers formed. As the polymerization process is governed by a cGMP-quadruplexation, naturally the G-content in the oligomers formed is very high. However, inside the thermal non-equilibrium setting (colored circles) cCMPs nucleotides are incorporated more readily into the strands compared to the pure drying protocol at isothermal conditions (grey circles). The lines here are guides to the eye and not finite element simulations as in the main text. (b) The thermal pore increases the formation of mixed sequences and up to doubles the rate of incorporation of C-nucleotides independently for all tested initial monomer compositions and concentrations.

Fig. S16.



SI-FIG. S16. AlmpdA Polymerization is Enhanced by the Thermal Pore For active, linear and pyrophosphate oligomers (all lengths summed) the bottom of the pore (black) yielded a stronger polymerization result than the respective bulk control (grey) for all starting monomer concentrations (2.5/20/300 mM AlmpdA). The percentages of yield-enhancement by the non-equilibrium conditions of the pore can be found in SI-Table S7. Error bars indicate 50 % error estimates (see SI-section VIII.2)

Table S7.

Initial AlmpdA Concentration	Active Oligomers	Linear Oligomers	Pyrophosphate Oligomers	Sum of all Oligomer Types
2.5 mM	42 %	491 %	86 %	85 %
20 mM	1015 %	928 %	2378 %	2063 %
300 mM	77 %	284 %	346 %	213 %

SI-TAB. S7. Percentages of Yield-Enhancement by the Non-Equilibrium Conditions of the Pore in Comparison to the Bulk Experiment For active, linear and pyrophosphate oligomers (all lengths summed) the bottom of the pore yielded a stronger polymerization result than the respective bulk control for all starting monomer concentrations (2.5/20/300 mM AlmpdA, see SI-Fig. S16).

XI. SI-MOVIES

SI-Movies can be downloaded from: Dirscherl, Christina Felicitas and Braun, Dieter: *Supplementary Datasets for the Paper "A heated rock crack captures and polymerizes primordial DNA and RNA"*. 2022. Open Data LMU. DOI: <https://data.ub.uni-muenchen.de/351/>

Movie S1 (separate file). Pore Filling with Help of Low Viscosity Oil

The sample mixture is filled into a thermophoretic pore, which has beforehand been filled with very low viscosity Novec oil to allow complete filling of the pore without introducing any air bubbles. Novec oil was checked in a separate experiment to not change the polymerization behavior.

Movie S2 (separate file). Pore Filling with an Air-Water Interface

The sample mixture was filled into an air-filled thermophoretic pore from its top until it filled the upper 4/5 of the chamber volume, the lowest fifth was left air-filled to create the liquid-gas interface.

Movie S3 (separate file). Pore Building Procedure

A thin Teflon foil was placed between two transparent sapphires. The sapphires were lined with two heat-conducting graphite foils to ensure a good thermal connection to an aluminum plate at the back and to the resistance rod heaters at the front. The layers were screwed with a steel frame to the back plate, the heater was screwed to the front sapphire. This sandwich is screwed to a waterbath-cooled aluminum block with another graphite foil in between. Four microfluidic teflon tubings were connected with fittings and ferrules to the sapphire back wall of the chamber, which has holes of 1 mm diameter. These tubings served as inlet and outlet for the introduction of the liquid sample.

Movie S4 (separate file). Freeze Extraction Procedure

After the run time of the reaction in the thermal gradient, we turned off the front heating, which lead to a rapid drop in temperature and finally to the freezing of the pore contents. We removed the entire pore from the setup and placed it in the -80°C freezer for 30 min. Then the sapphire-teflon-sapphire sandwich was unscrewed from the metal holders. The sandwich was placed on an aluminum block cooled to -80°C to prevent melting. The sandwich was opened, and the Teflon was removed using a razor blade. Only the frozen liquid content remained on the sapphires. We cut this into five stripes (for experiments of Fig. 1 and Fig. 2) or three stripes (for experiments of Fig. 3) of similar volume and slid the sapphire stripe by stripe over onto a 45°C aluminum block to melt the frozen sample stripe by stripe. To ensure that two adjacent stripes were not inadvertently mixed during the stripewise thawing, we held a hydrophobic barrier (glass cover slide wrapped with Teflon foil) between each stripe (see SI-Fig. S4). The contents of each thawed stripe were pipetted into different low-binding Eppendorf tubes.

Movie S5 (separate file). Thermogravitational Accumulation in a Water-Filled Pore

An out-of-equilibrium hydrothermal pore can localize and concentrate molecules. The thermal gradient induces two physical phenomena inside the pore: first, the bulk solution undergoes a circular convection motion due to the heat-induced density differences within the liquid. Second, the dissolved molecules within the liquid experience thermophoresis, a drift along the temperature gradient (for DNA/RNA molecules towards the colder side of the pore). The superposition of these two forces leads to a concentration increase of molecules at the bottom cold corner of the pore. The resulting accumulation of molecules is balanced by diffusion, seeking a homogeneous concentration.

Movie S6 (separate file). Accumulation and Wet-Dry Cycles in a Pore with Air-Water Interface

In a pore with an air-water interface subjected to a temperature gradient, convection and thermophoresis are joined by evaporation at the hot side and recondensation at the cold side of the pore. In addition to the downward accumulation, the solutes undergo a wet-dry cycling: RNA molecules are deposited in layers on the hot side and are rehydrated by growing water droplets at the cold side, which re-enter the main fluid phase and shift the location of the water-air interface over time.

XII. SI-DATASETS

SI-Datasets can be downloaded from: Dirscherl, Christina Felicitas and Braun, Dieter: *Supplementary Datasets for the Paper "A heated rock crack captures and polymerizes primordial DNA and RNA"*. 2022. Open Data LMU. DOI: <https://data.ub.uni-muenchen.de/351/>

Dataset S1 (separate file). Self-coded LabVIEW Program for Mass Calculation

The masses of the two types of oligomer products formed in the 2',3'-cyclic polymerization were calculated to the fourth charge state using a self-coded LabVIEW program. The resulting masses are used for further analysis and are displayed in SI-section VI.3.

Dataset S2 (separate file). Self-coded LabVIEW Program for Temperature Calculations for Thermophoretic Pores

To calculate the inner temperatures of the chambers, we measured the temperatures on the outside of the sapphires with a temperature sensor and used the steady-state linear heat equation and the conductivities of water 0.60 W/mK (at 20°C) and of sapphire 23 W/mK to calculate what temperature this translates to on the inside of the pore.

Dataset S3 (separate file). Self-coded LabVIEW Programs for Product Peak Integration and Isotope Pattern Matching

For the quantification of polymerization products from 2',3'-cyclic monomers we used two self-coded LabVIEW programs to integrate the product chromatogram peaks and to check the isotope distribution.

Dataset S4 (separate file). Isotope Pattern Documentation

Screenshots of the Isotope Patterns for all detected strand lengths and base compositions for the 10 mM 2',3'-cCMP / 50 mM 2',3'-cGMP experiment for both, thermophoretic pore and drying at 40°C. The theoretical isotope pattern is displayed in green and was compared with the ESI-TOF-measured isotope pattern in white (closer description to the software can be found in [1]).

Dataset S5 (separate file). Comsol Simulation Files for all Theoretical Calculations

Numerical simulations for the robustness sweep, monomer accumulation, AlmpdA accumulation+polymerization for thermophoretic pores and bulk control, 2',3'-cyclic accumulation+polymerization for thermophoretic pores and drying control, 2D-longtime monomer accumulation with and without feeding and 0D-longtime 2',3'-cyclic polymerization with and without feeding.

Dataset S6 (separate file). 2',3'-cyclic Polymerization Rate Equations and Self-Coded LabVIEW Program for their Calculation.

The rate equations for all strands of the 2',3'-cyclic polymerization are generated with length- and sequence-dependent on-rates are created with a self-coded LabVIEW program. The resulting equations are used in the combined accumulation and polymerization simulations.

SI-REFERENCENS

1. Dass AV, Wunnava S, Langlais J, von der Esch B, Krusche M, Ufer L, Chrisam N, Dubini R, Gartner F, Angerpointner S, Dirscherl CF, Rovó P, Mast CB, Šponer JE, Ochsenfeld C, Frey E, Braun D. RNA Oligomerisation without Added Catalyst from 2',3'-cyclic Nucleotides by Drying at Air-Water Interfaces. *ChemSystemsChem*. 2022;e202200026.
2. Kanavarioti A. Dimerization in highly concentrated solutions of phosphoimidazolidine activated mononucleotides. *Orig Life Evol Biosph*. 1997;27(4):357-376.
3. Ertem G, Ferris JP. Synthesis of RNA oligomers on heterogeneous templates. *Nature*. 1996;379(6562):238-240.
4. M.K. Łącki, D. Valkenburg, M. Startek, IsoSpec2: Ultrafast Fine Structure Calculator. *Anal Chem*. 92(14):9472-9475 (2020).